ROOF TOP HARVESTING AND STORMWATER DISPERSEMENT OVER THE EDWARDS AQUIFER RECHARGE ZONE: A RETROFIT FOR TREATMENT OF PREVIOUSLY UN-TREATED IMPERVIOUS COVER

A City of San Antonio, Edwards Aquifer Protection Venue program funded project

FINAL REPORT PREPARED FOR:

City of San Antonio
Parks and Recreation Department
Edwards Aquifer Protection Program

and

San Antonio River Authority





BRIAN G. LAUB MELISSA GARCIA LANI MAY

The University of Texas at San Antonio San Antonio, Texas





October 31, 2022

EXECUTIVE SUMMARY

Expanding urban development in San Antonio and surrounding communities poses a threat to the region's aquatic resources, including the Edwards Aquifer. Urban development impacts water resources by increasing stormwater runoff and pollutant delivery to downstream waters. There is growing interest in using green infrastructure, or low impact development (LID) facilities, to help manage stormwater runoff and pollutant loading from newly constructed and existing urban areas, but there exists uncertainty as to feasibility and benefits of implementing such facilities in multi-use urban environments, such as university campuses.

In 2017, funding was obtained through the City of San Antonio's Edwards Aquifer Protection Venue Program to retrofit 9.7 acres of impervious cover on the University of Texas at San Antonio (UTSA) main campus with LID facilities. The LID facilities were intended to reduce peak flooding and pollutant transport downstream during runoff events on the campus, which is located over the Edwards Aquifer recharge zone. The project also aimed to serve as a demonstration project for the feasibility of implementing LID facilities on a university campus. The LID facilities installed included cisterns, a bioretention basin, a grassy channel and a bioswale, connected through flow pathways in a treatment train approach. A research study analyzed the flow attenuation and pollutant removal effectiveness of the bioretention basin.

Construction of the LID facilities was successfully completed in November 2020. The LID facilities were placed in a central area of campus, which transformed a lightly used mowed lawn and stormwater conveyance channel into a landscaped retention basin and bioswale that serve as an intermittent water feature in a highly trafficked area of campus. Signs placed near each LID facility inform students and campus visitors about the operation of LID facilities and their role in water quality protection and conservation of the Edwards Aquifer and other aquatic resources.

Together, the LID facilities can hold nearly 400,000 gallons of stormwater runoff, which is then released slowly as irrigation water if captured in cisterns, or infiltrates into the soil of the bioretention basin and bioswale for water filtering. The retention and slow release of stormwater runoff substantially attenuated flood peaks in downstream channels.

The bioretention basin significantly reduced loads of *E. coli* bacteria, demonstrating, together with reductions in first flush concentrations of sediment, nitrate, and copper, a pollutant removal function. Although loads of total dissolved solids and first flush concentrations of arsenic increased after passing through the bioretention basin, water exiting the basin flows through an unmowed grassy channel and a constructed bioswale. The treatment train effect of this series of LID facilities likely further improves water quality flowing downstream away from campus.

Overall, the LID facilities were successfully integrated into the university campus and are now serving as functional green spaces. The LID facilities increase hydrologic retention, pollutant filtering, and educational opportunities compared to the conditions existing prior to project implementation. The project shows that LID facilities can provide similar benefits to other university campuses and are feasible to implement.

Introduction

Expanding urban development is one of the primary threats to aquatic ecosystems and clean water supplies in regions experiencing rapid population growth (McGrane, 2016). As urbanization proceeds, roads, parking lots, roof tops, and other impervious surfaces replace woodlands, forests, wetlands, and other green spaces (Brabec, Schulte, & Richards, 2002). Replacement of green spaces with impervious surfaces reduces infiltration and evapotranspiration and increases surface runoff during precipitation events, routing stormflow directly to stream channels (Leopold, 1968). Precipitation transferred to surface runoff bypasses the natural retention, transpiration, and filtering processes that occur during infiltration, interaction with vegetation, and movement through soils toward stream channels. The increase in surface runoff at the expense of infiltration leads to flashier flow patterns in streams and rivers due to the decreased lag time between precipitation and flooding response, in combination with increases in total runoff volume and peak flood magnitudes (Leopold, 1968; Paul & Meyer, 2001). Downstream ecosystems are also impacted by increased water temperatures, increased nutrient and pollutant runoff, and degraded water quality, often including increased concentration of bacterial indicators such as E. coli (Arnold, Boison, & Patton, 1982; Bannerman, Owens, Dodds, & Hornewer, 1993; Huber, Welker, & Helmreich, 2016; Morisawa & LaFlure, 1979; Paul & Meyer, 2001). Pollution loads in stormwater also pose a contamination threat to groundwater systems, especially in quick-recharging aquifers where filtration through vegetation and soils is minimal (Andrews, Schertz, Slade, & Rawson, 1984).

Given the strong impact of urban development on flooding, river ecosystem health, and water quality, substantial resources and effort have been invested in developing methods for mitigating impacts of urban development and restoring impacted aquatic environments. The suite of techniques applied to help manage impacts from urban development are termed green and blue infrastructure or low impact developments (LID). Example LID facilities include cisterns, green roofs, and bioretention basins. The common objectives behind LID facilities are to increase hydrologic retention and increase infiltration and associated water filtering processes, though not all features target both objectives. For example, cisterns capture and store runoff, usually from rooftops, for later use, increasing hydrologic retention, but have minimal water filtering ability. Bioretention basins are constructed depressions partially filled with sand and soil and planted with usually native vegetation. Bioretention basins are designed to increase hydrologic retention by capturing and ponding stormwater runoff and promote water filtration by allowing the captured runoff to filter through the sand and soil material and interact with vegetation. A common approach when implementing LID facilities in urban landscapes is to apply multiple features in series in what is termed a treatment train. For example, surface runoff from impervious surfaces such as rooftops may be routed through a rain garden at the outlet of rooftop drains, then into a drainage channel that feeds into a bioretention basin, and finally a downstream grassy swale before discharging into a stream or river channel.

Implementation of LID facilities in developing urban landscapes can help protect downstream ecosystems, people, and urban infrastructure in several ways. By increasing hydrologic retention and infiltration, LID facilities help to delay the routing of stormwater runoff downstream, which can decrease peak flood magnitudes and lower flooding risk. Many aquatic species, particularly those that live in aquifers, are sensitive to degraded water quality. Degraded water quality also impacts human water supplies, as well as recreation and fishing opportunities. By helping to increase filtration of stormwater runoff before the water enters groundwater systems or stream channels, LID facilities can help protect aquatic species as well as human health. Properly landscaped LID facilities can also provide economic, aesthetic, and sociological benefits. For example, healthy, protected green spaces provide multiple benefits to neighboring properties, including higher value, reduced costs of heating and cooling, and a greater sense of wellbeing for residents compared to similar properties not near green spaces (Gwinn et al., 2018).

The city of San Antonio and the surrounding communities represent an area where there is strong interest in using LID facilities to help mitigate impacts to aquatic resources as urban development grows. San Antonio is the seventh largest city in the U.S. and one of the fastest growing. The city is in a region prone to intense precipitation events and severe flash flooding, which can be exacerbated as urban development and associated impervious surfaces expand. In addition, the city derives the majority (51.2%) of municipal water supply from the Edwards Aquifer (https://www.saws.org/your-water/management-sources/). The Edwards Aquifer is a quick-recharging karst aquifer, making it vulnerable to contamination from polluted surface runoff (Masoner et al., 2019). The Edwards Aquifer is also home to several federally-protected endemic species that are sensitive to water quality alterations (Bowles & Arsuffi, 1993). Groundwater contamination at regulated facilities around San Antonio (TCEQ, 2020), as well as increasing nitrate amounts in the aquifer (Musgrove et al., 2016), indicate urban development poses a strong threat to sustainability of the Edwards Aquifer water supply.

Recognizing the threat to aquatic ecosystems, particularly the Edwards Aquifer, posed by expanding urban development, the City of San Antonio has implemented several mitigation programs using voter-approved funding, known as Proposition 1 projects. One component of the Proposition 1 program was purchasing of land in Bexar County over the Edwards Aquifer recharge zone for protection. Another component, which funded the current project, was investment in research and demonstration projects to better understand how LID facilities and other mitigation approaches could most effectively be implemented to help reduce impacts from already developed urban areas and areas slated for future development outside the recharge zone of Bexar County.

In this project, a series of LID facilities were constructed on the University of Texas at San Antonio (UTSA) main campus, which is located over the recharge zone of the Edwards Aquifer. The LID facilities, which included cisterns, a bioretention basin, and a bioswale were implemented in series as a treatment train. A research program was also undertaken to

determine whether the bioretention basin mitigated downstream peakflows and removed pollutants from stormwater runoff, including nutrients, metals, sediments, and bacterial indicators, more effectively than the pre-construction condition, which consisted of a mowed grassy stream channel. The current report describes the design and implementation of the LID facilities on the UTSA campus, the general current condition and operation of the LID facilities two years after construction, and the implementation, results, and conclusions from research on the bioretention basin. An associated business plan, submitted separately from this report discusses costs, challenges, benefits, and lessons learned from project implementation, as a guide for similar institutions considering whether and how to implement LID facilities.

Project Implementation

The LID facilities on the UTSA campus were designed to treat 13.7 acres of campus containing 9.5 acres of previously untreated impervious cover, including parking lots, roadways, sidewalks, and rooftops. The LID facilities were connected through flow pathways into a treatment train (Figure 1), and included two cisterns, a bioretention basin, an unmowed grassy channel, and a bioswale.

Cisterns

Two 9,500 gallon cisterns were placed in an interior breezeway between the Convocation Center and the Intercollegiate Athletic Building (Figure 2). The cisterns capture rooftop runoff from both buildings. The location provided immediate access to rooftop drains and was also in a highly visible location on campus, which promoted informative signs and visibility of the cisterns. Water collected in the cisterns is used to irrigate nearby green spaces. When the cisterns fill, the excess water from rooftop drains flows into sidewalk surface drains and eventually into the bioretention basin.

Bioretention Basin

The bioretention basin is a constructed depression filled with a sand and soil media, which is designed to pond water during runoff events and allow the ponded water to filter through the sand and soil media over a period of 12-72 hours. The basin was also planted with native plants, with different species at different elevations corresponding to the expected soil moisture conditions. The final constructed basin is divided into a forebay and a north and south basin, covering an area of approximately 0.5 acres and holding an approximate volume of 374,000 gallons (Figure 3). The forebay and north basin are connected, and receive water from the upstream channel and from the HEB Student Union (HEB SU) rooftops and adjacent sidewalks. The north basin is divided from the south basin by an earthen berm, with an overflow pipe in the berm connecting the two basins. Thus, the south basin receives water overflowing the north basin, as well as water from the Convocation Center rooftop and walkways and other surfaces primarily to the east of the basin.

The final designed footprint and depth of the basin was determined by a need to hold 80% of the runoff volume from a 1.5-inch rain event over the contributing area of the basin

while preserving existing trees and infrastructure to the extent possible. The pre-construction condition at the bioretention basin location was a mowed lawn with several patches of live oak trees on the sides and a channel running through the center that conveyed stormwater downstream during precipitation events (Figure 4). The channel continued north of the bioretention basin location and collected water from areas upstream of the bioretention basin location, including parking lots, tennis courts, and rooftops. Water also entered the channel through drains from the Convocation Center rooftops, the HEB SU rooftop, and adjacent sidewalks. An underground water pipe ran perpendicular to the channel between the Convocation center and the HEB SU.

The lawn at the bioretention basin location provided an ideal location for basin construction, because it was an existing open space that was crossed by an unofficial pedestrian path but was not heavily used as a recreational or gathering area by the campus community. However, fitting a basin of sufficient size to hold the designed storm volume, while preserving existing trees and underground infrastructure required expanding the footprint and depth in several locations compared to the initial design plans. Other important considerations in basin design were to minimize foot traffic across the basin to prevent damage to plants, ensuring the slope into the basin was not a safety hazard, and providing an aesthetically pleasing space given the location near the center of campus. The planting plan helped to address these issues, in that larger trees and shrubs were planted at key potential access points and across the berm to discourage foot traffic and prevent pedestrians from interacting with the steep slopes of the basin.

Construction of the basin followed the San Antonio River Authority (SARA) LID technical design guidance manual (SARA 2019). The excavated basin was lined with an impermeable liner, and perforated pipe was placed in the bottom of the basin to drain water that filtered through the overlying sediment and soil layers (Figure 5). Design documents called for a 1.25foot layer of 1-inch washed gravel (#57 stone) to be placed on the liner and around the underpiping. Delivered base rock was unwashed, heavily silted, and more chipped than specifications, but was still accepted for use in the basin. Immediately atop the gravel, a barrier layer of 2-inch washed sand media, with grain size distribution comparable to washed concrete sand was applied. A layer of soil biomedia mix, with design specifications of 3-feet minimum depth, consisting of 85-88% washed coarse sand, 8-12% fines passing a #270 sieve, and 2-5% organic matter was placed atop the sand barrier layer. The biomedia mix was tested to determine whether it met design specifications, and several mixes did not meet specifications and were rejected. The process of finding biomedia mix that met design specifications delayed construction progress. The biomedia mix was covered with a 4-inch layer of shredded hardwood mulch. One exception was the forebay, which was lined with cobbles, because the forebay received runoff from the upstream channel as well as the HEB SU, so was an area of high flow energy, and the cobbles were placed to help reduce erosion.

Once the biomedia was in place, vegetation was planted in and around the basin. All plantings were native species and were chosen according to the soil moisture conditions expected at different elevations in and around the basin as well as aesthetics. Plants adapted to

periodic submergence and flooding were planted in the bottom of the basin and included Texas frogfruit (*Phyla nodiflora*), inland sea oats (*Chasmanthium latifolium*), Berkeley sedge (*Carex tumicola*), and meadow sedge (*Carex perdentata*). Lower to mid-elevation surfaces on the slopes of the basin included grasses such as bull grass (*Muhlenbergia emersleyi*), pink muhly (*Muhlenbergia cappilaris*), and Lindheimer's muhly (*Muhlenbergia lindheimeri*). Drought-tolerant plants were chosen for the tops of the basin, above the expected ponding depth, and included shrubs such as turk's cap (*Malvaviscus arboreus var. drummondii*), dwarf Yaupon holly (*Ilex vomitoria*), agarita (*Berberis trifoliata*) and various yucca and agave species, as well as larger trees including thornless retama (*Parkinsonia x 'Desert Museum'*). Numerous other species were also planted in part due to aesthetic purposes, such as Greg's mistflower (*Conoclinum gregii*), which is attractive to butterflies.

The basin underpiping drained to a concrete sump housing, in which a pump was installed to convey water that had passed through the basin soils downstream. The pump was needed to convey water over the edge of the basin, otherwise water would have stayed ponded in the basin soils indefinitely. The pump is operated by float-triggered switches designed to turn on when water fills the sump to a designated level and turn off when the pump drains water to a lower designated level. The sump housing and pump were a modification to the initial design, which called for a gravity drain out of the basin. Constructing the gravity drain would have required boring a tunnel through bedrock, and although geotechnical assessments indicated the tunnel was feasible, the sump housing and pump reduced construction costs substantially, though the pump will require long-term maintenance. In addition to the sump outlet, water is conveyed out of the south basin downstream via an overflow structure if the basin reaches full storage capacity during a runoff event.

Grassy Channel and Bioswale

Water pumped out of the bioretention basin or overflowing the basin flows downstream into two further LID facilities comprising the overall treatment train, one being an unmowed grassy channel (Figure 6), and the other a constructed bioswale (Figure 7). The area where the grassy channel and bioswale were constructed was the same drainage channel flowing through a maintained lawn that existed prior to the bioretention basin construction, but further downstream. The grassy channel was not modified as part of this project, except that mowing in the existing channel was discontinued. The bioswale consists of one small basin constructed within the previous channel, plus a series of small pools separated by limestone blocks just upstream of the basin (Figure 7). The basin is a smaller version of the bioretention basin, with an impermeable liner, underpiping, plus a gravel layer beneath sand and soil fill. The bioswale was also mulched after planting with some of the same native species used in the bioretention basin. Water that drains through the bioswale exits into a downstream channel, which flows for approximately 1 km through further grassy sections on the UTSA campus and an adjacent neighborhood before discharging into Leon Creek.

Informational Signs

Signs describing the operation and purpose of the cisterns, bioretention basin, and grassy channel and bioswale were placed at several locations (Figure 8). The signs provide students and visitors to campus information about the LID facilities, thus raising awareness about the importance of stormwater management for protecting aquatic resources.

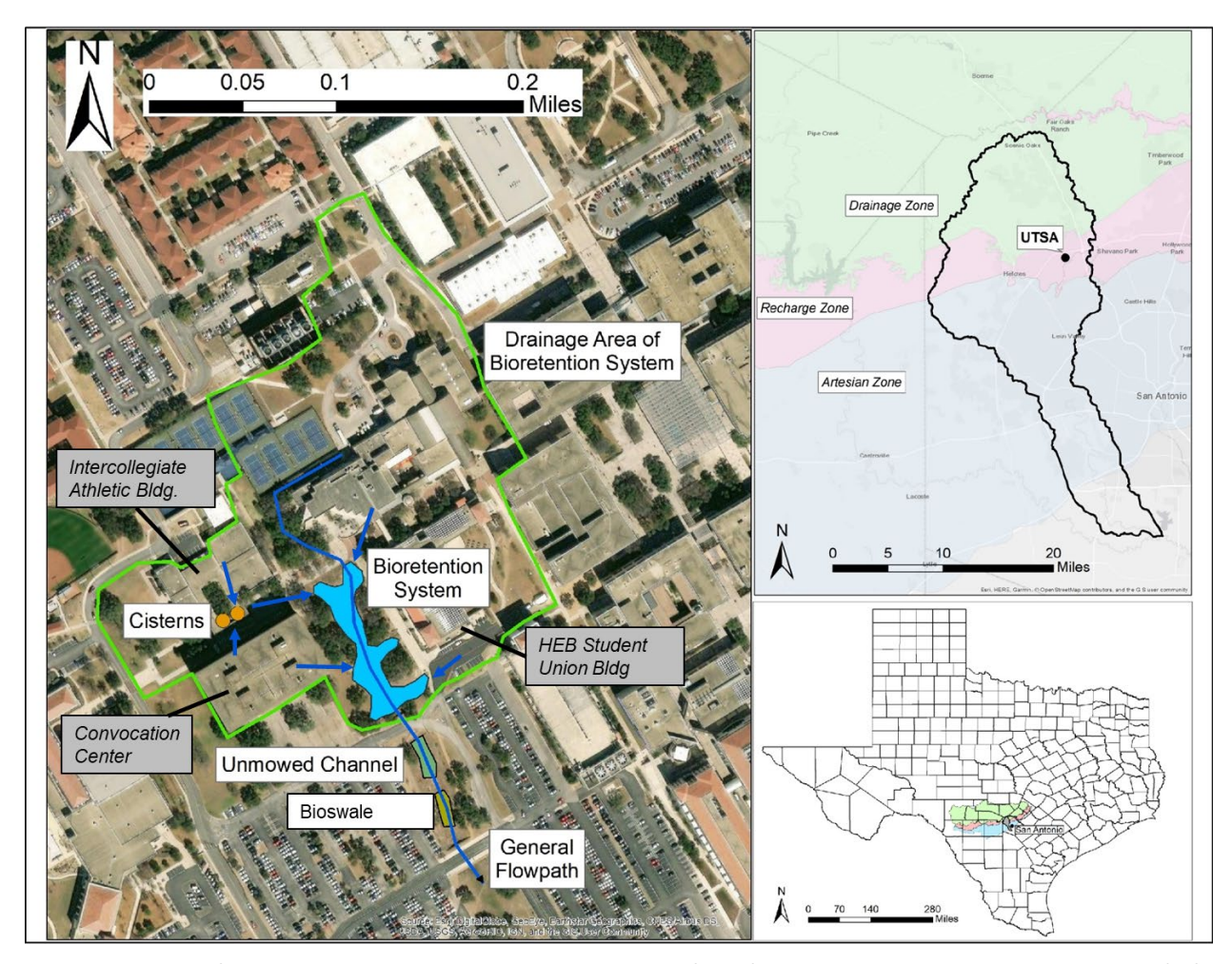


Figure 1. Map of the UTSA campus showing the location of LID facilities implemented in this project (left panel), as well as some campus buildings. The LID facilities were connected via flow pathways, shown in blue arrows, into a treatment train. The right panels show the location of the UTSA campus over the Edwards Aquifer recharge zone within the Leon Creek watershed (top) and the Edwards Aquifer region within the state of Texas (bottom).



Figure 2. Picture showing the two cisterns in the breezeway between the Convocation Center and Intercollegiate Athletic Building, adjacent to a major walkway through campus.



Figure 3. Map of the constructed bioretention basin, showing drainage pathways, samplers, and other features.



Figure 4. Before-after photos looking downstream, showing the mowed channel in the preconstruction condition and the north basin of the bioretention basin two years post-construction.



Figure 5. Photograph showing the impermeable liner and basin partially filled with sand and biomedia mix.



Figure 6. Photograph showing the unmowed grassy channel. Picture orientation is looking downstream toward the bioswale.



Figure 7. Photograph showing the bioswale. Picture orientation is looking upstream toward the unmowed grassy channel and bioretention basin.



Figure 8. Pictures showing several of the information signs posted near the LID facilities. The bottom-left picture shows details of the layers contained in the bioretention basin.

Bioretention Basin Effectiveness Study Methodology

Sampling Approach

Peakflow mitigation and water quality performance assessment focused on the bioretention basin, because it was the largest and most costly LID feature implemented in the treatment train. The approach taken to assess peakflow mitigation was to compare downstream flow patterns with and without the basins installed, with hydrographs constructed using data on water level changes in the basin. The approach taken to assess water quality treatment performance of the bioretention basin was twofold: 1) water quality entering the constructed bioretention system was compared to water quality leaving the system, and 2) the effectiveness of the bioretention system was compared to water treatment effectiveness of the mowed grassy channel that existed prior to bioretention basin construction. Treatment effectiveness of the pre-construction channel was assessed by comparing water quality sampled upstream and downstream at similar locations to the current input and output of the bioretention basin. Thus, we were able to assess removal of pollutants from the bioretention basin and compare treatment effectiveness of the basin to treatment effectiveness of the pre-construction grassy channel.

Sampling occurred during stormwater runoff events, because the bioretention basin was normally dry but captured runoff during storm events from an upstream drainage area, stored the water temporarily, and allowed the stormwater runoff to filter through a soil biomedia mix before being discharged downstream. Three types of sampling data were collected during runoff events both pre and post-construction. Water depth in the two basins and in the sump of the bioretention system was monitored continuously post-construction. Flow depth was also monitored continuously at an upstream (site A) and downstream (site B) location in the grassy channel pre-construction, at locations roughly equivalent to the upstream and downstream ends of the constructed bioretention basin (Figure 9). Temperature was also recorded continuously at these same locations both pre- and post-construction, and in several channels and outfall pipes pre-construction. Water samples during runoff events were collected from these same locations, with a goal of capturing aliquots across the entire runoff event (i.e., flow-paced sampling), including first flush aliquots and up to three separate follow-on aliquots. All aliquots were then taken to the laboratory for measurement of analytes. Aliquots were not composited, meaning that analytes were measured for up to four aliquots for each event at each site.

Water sample collection

At sites A and B pre-construction and at the north and south basins and sump outfall post-construction, autosamplers (ISCO model 3700) were paired with a flow meter (ISCO Signature model) to enable flow-paced sampling (Figure 10). The autosamplers were configured to begin sampling upon receiving a flow detection signal from the flow meters for the first flush. In the pre-construction channel, the autosamplers then entered a "flow paced" program,

collecting follow-on aliquots upon receiving a signal from the flow meter that a specified amount of discharge had passed, equivalent to a volume that would pass in a 15-minute period if the channel was 50% full by depth. In the post-construction basins and outfall sump, samplers were programmed to collect follow-on aliquots once an hour for up to 3 hours after the first flush. Time-paced sampling was used post-construction because water was ponded in the basins rather than flowing through the basins, as in the pre-construction channel. Autosamplers were set to collect an aliquot consisting of five one-liter (L), acid-washed bottles for each flush, to allow for sufficient volume for testing all analytes. A maximum of 20 L were collected at each site, equivalent to one first flush aliquot and three follow-on aliquots in any given storm event, as the autosamplers have a maximum capacity for 24 1-L polypropylene bottles; the last four one-L bottles were not used.

In the pre-construction channel, the autosamplers were programmed to cease collecting when one of two conditions was met. The first was when four five-L aliquots had been collected, the maximum capacity. The second was when two hours had elapsed since the last five-L aliquot was collected, signifying that the flow event ended before four aliquots could be collected.

Efforts were made to retrieve sample bottles from the autosamplers as soon as possible. Samples that were retrieved more than 24 hours after collection were not processed for time-sensitive analytes. All collection bottles were transported to the UTSA Science Research Lab (SRL) and either processed immediately or stored in a refrigerator for later processing.

There were several locations and times when manual grab samples were collected in replacement of collection by autosamplers. In the pre-construction sampling phase, grab samples from Convocation Center and HEB SU outfalls were collected opportunistically. This was accomplished by submerging three labeled one-L bottles with mouths facing away from the direction of flow. In the post-construction phase, sump grab samples were collected for multiple events due to periodic issues with the sump pump not operating as designed. The pump issues were eventually resolved, and the pump is now operating correctly, but issues during sampling interfered with correct operation of the sump autosampler.

Storm events that occurred less than 72-hours after a previous storm event were not sampled in this study. In other words, the study required a 72-hour antecedent dry period for a storm event to be sampled. This requirement was in accordance with Environmental Protection Agency (EPA) guidance under 40 CFR §122.21(g)(7)(ii). A flow event was defined as any detected flow depth that was sufficient to trigger a first flush collection.

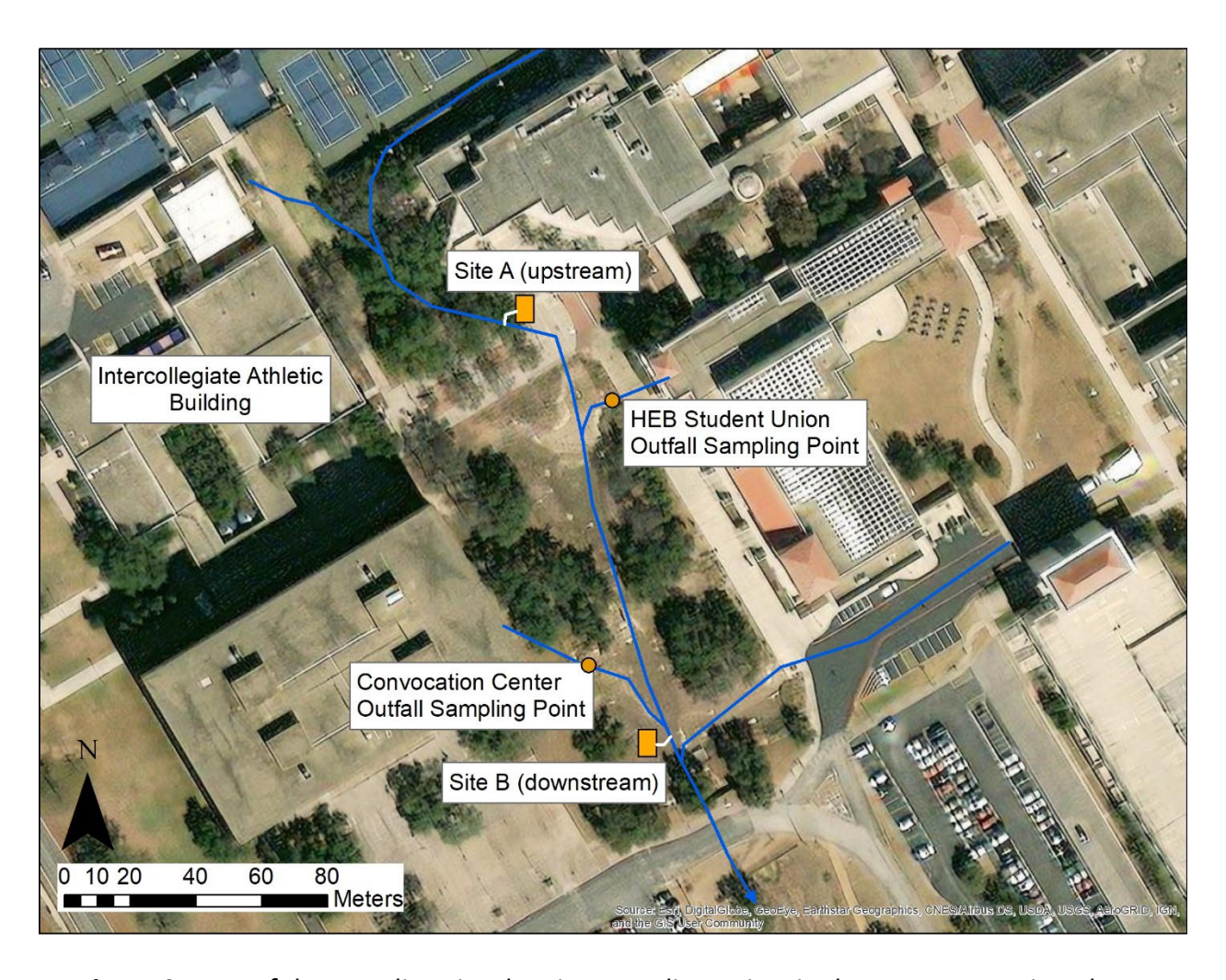


Figure 9. Map of the sampling site showing sampling points in the pre-construction phase.



Figure 10. Picture of the automatic water sampler on the left and flow meter on the right.

Autosampler Locations

In the pre-construction channel, autosamplers were installed at an upstream (site A) and downstream (site B) location (Figure 9). The upstream water intake tube and flow-level detection line were installed in a rectangular concrete culvert that ran under the Paseo Principal walkway. The primary stormflow inputs to site A came from roadways, parking lots, and the tennis court complex north of the channel. The downstream water intake tube and flow-level detection line were installed in the middle of the mowed-grass channel on a concrete pad. Stormflow inputs to site B included all water that passed site A, plus rooftop drainage from the Convocation Center and HEB SU and adjacent sidewalks.

In the post-construction system, autosamplers were placed to sample the north basin, south basin, and comingled water which had filtered through each basin at the sump outlet (Figure 3). The water intake tube and flow-level detection lines for the north and south basins were each secured to large boulders at the approximate low-point of each basin. Stormflow

inputs to the north basin came from the same upstream drainage area that flowed through site A pre-construction and from the HEB SU rooftop and surrounding sidewalks. Stormflow inputs to the south basin included overflow from the north basin when the north basin filled, plus runoff from the Convocation Center rooftop and lawns and impervious surfaces to the east of the basin. The water intake tube and flow-level detection lines for the sump outlet sampler were placed in the concrete sump housing, at a depth below the level at which the pump turned off, such that the intake openings were always submerged. Water draining through biomedia mix of both the north and south basin entered the same underpiping, such that water sampled from the sump outlet represented comingled treated water from both basins.

Flow meter configuration

The flow meters (ISCO Signature model) recorded water depth every 5 minutes, with the exception of the upstream (site A) pre-construction meter, which recorded depth every 15 minutes from installation to 6 November 2018. Water depth was converted to water volume differently for the pre-construction channel and post-construction basins and sump. Depth in the basins was converted to volume using a depth to volume rating curve based on the surveyed basin geometry (Figure 11). The forebay volume was ignored in these calculations. The initial plan for calculating the volume of water passing through the sump was to use a depth-volume curve, with total volume determined by the number of times the sump was emptied by the pump. However, sump volume for individual events proved difficult to calculate due to inconsistent operation of the pump and a near-continuous movement of water into and out of the sump. Therefore, volume passing through the sump for each sampled event was assumed equal to the total volume collected in the bioretention basins.

In the pre-construction channel, depth was converted to flow rate by multiplying measured cross-sectional area with an estimated flow velocity (m/s) from Manning's formula:

$$Q = AV = A \frac{1}{n} R_h^{2/3} S^{1/2},$$

where Q is flow rate in m/s, A is channel cross-sectional area in m, V is flow velocity in m/s, n is a roughness coefficient, R_h is the hydraulic radius in m, and S is the slope. Roughness was estimated using standard tables for different channel types, in this case a grassy channel. Cross-section area and hydraulic radius was obtained from the measured cross-section profile and slope from the surveyed channel elevation change.

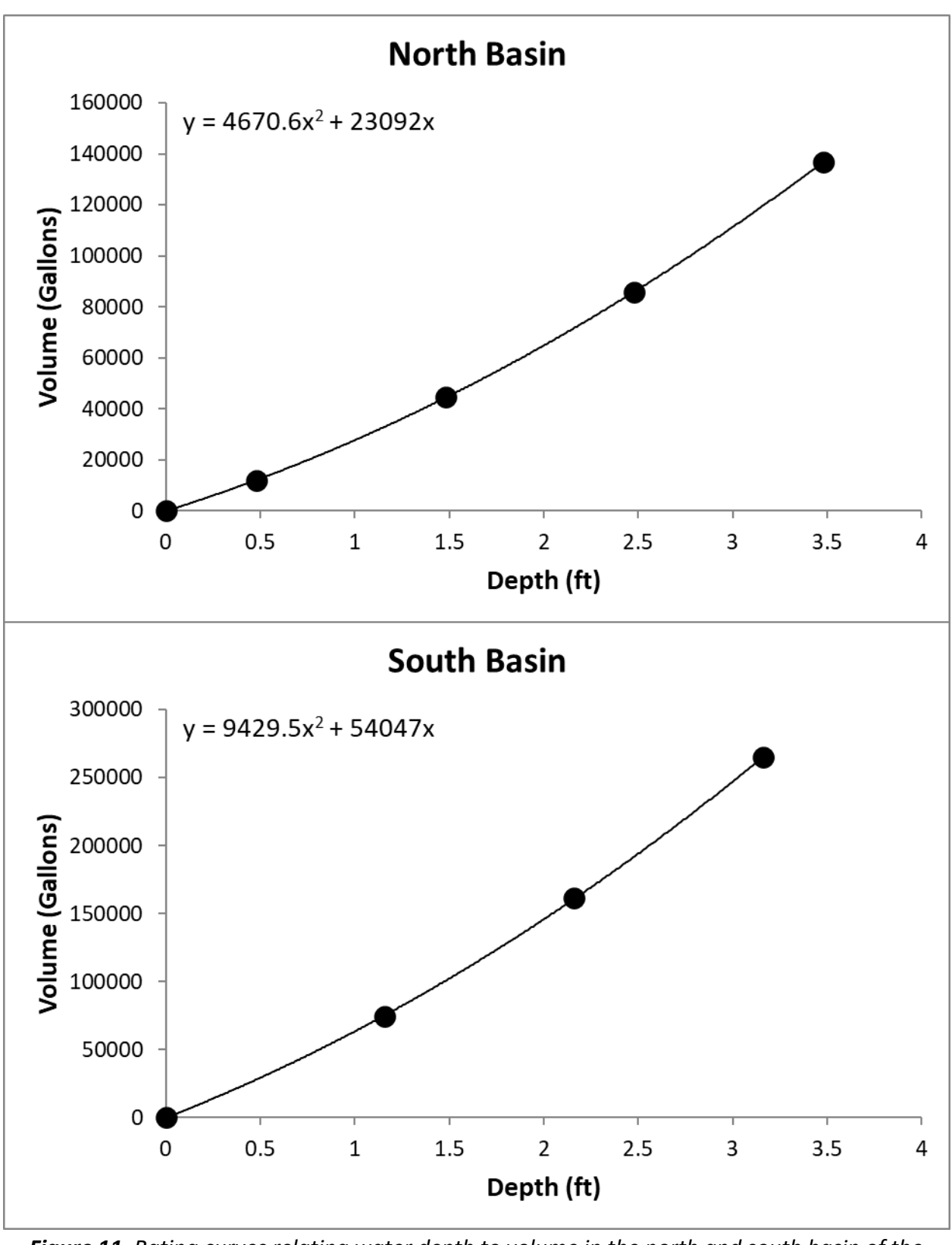


Figure 11. Rating curves relating water depth to volume in the north and south basin of the bioretention basin.

Temperature data collection

To collect temperature data, water-proof temperature loggers (HOBO Pendant MX2201, ONSET) were installed at all sampling locations. Loggers were set to record temperature every minute. In addition, loggers were installed near, but outside, the channel and basins to record ground-surface temperatures prior to and during storm events.

Water sample analysis

Multiple analytes were measured for each collected flush (Table 1), generally grouped into physicochemical parameters, nutrients, metals, and other contaminants. Concentrations of metals, total organic carbon (TOC), and total petroleum hydrocarbons (TPHs) were measured by a third-party water quality analysis lab for both pre- and post-construction samples. The same third-party lab also analyzed pesticides and herbicides in pre-construction samples, TSS in pre-construction samples, and nutrients (NO₃, NO₂, TN, TP) in pre-construction samples and post-construction samples through 5 September 2021. Water from each flush was transferred to appropriate sample bottles and transported to the third-party lab on ice as soon as possible following sample retrieval.

Physicochemical parameters, including specific conductance, pH, and total dissolved solids (TDS) were measured in the UTSA lab using a calibrated probe (model YSI ProDSS). Total suspended solids (TSS) in post-construction samples were measured in the UTSA lab using a gravimetric approach, wherein a known volume of water was filtered through a pre-weighed glass-fiber filter, then the filter dried and re-weighed, and TSS calculated as mass of filtrate per volume filtered. Nutrients, other than TOC but including ammonia, were measured in the UTSA lab for all post-construction events starting on 29 September 2021. Nutrients were measured in the UTSA lab on a ThermoFisher Gallery Discrete Analyzer, which automates EPA standard photometric analysis of samples. Concentrations of E. coli were measured in post-construction samples in the UTSA lab using the IDEXX method, wherein sample water was mixed with an E. coli growth media, plated into multiple sample wells in a quantification tray, incubated at 37°C for 24 hours, and then observed under UV light to identify the number of sample wells containing E. coli colonies in the quantification tray. When possible, samples for E. coli were plated within 8 hours of autosampler collection, but always within 24 hours of autosampler collection. One post-construction event (29 April 2021) was sent to a third party testing lab instead of UTSA for *E. coli* sampling, though the method used was the same.

 Table 1. Sample analytes measured for this project.

Analyte type	Analyte	Analyte	Analysis	Method	
	-	abbreviation	Laboratory		
Physicochemical parameters	рН	рН	UTSA	Multiprobe	
	Specific conductance (μS/cm)	SC	UTSA	Multiprobe	
	Total Dissolved Solids (mg/L)	TDS	UTSA	Multiprobe	
Nutrients	Nitrate (mg/L)	NO ₃ -	Third Party/UTSA	EPA 300.0/EPA 353.1	
	Nitrite (mg/L)	NO ₂ -	Third Party/UTSA	EPA 300.0/EPA 354.1	
	Ammonia (mg/L)	NH ₃ -	UTSA	EPA 350.1	
	Total nitrogen (mg/L)	TN	Third Party/UTSA	EPA 351.3/EPA 351.2/EPA 353.1	
	Total phosphorus (mg/L)	TP	Third Party/UTSA	EPA 365.3/EPA 365.4	
	Total organic carbon (mg/L)	TOC	Third Party	SM 5310 B	
Metals	Silver (mg/L)		Third Party	EPA 200.7	
	Arsenic (mg/L)		Third Party	EPA 200.7	
	Barium (mg/L)		Third Party	EPA 200.7	
	Cadmium (mg/L)		Third Party	EPA 200.7	
	Chromium (mg/L)		Third Party	EPA 200.7	
	Copper (mg/L)		Third Party	EPA 200.7	
	Lead (mg/L)		Third Party	EPA 200.7	
	Selenium (mg/L)		Third Party	EPA 200.7	
	Zinc (mg/L)		Third Party	EPA 200.7	
	Mercury (mg/L)		Third Party	EPA 245.1	
Other	Total suspended solids (mg/L)	TSS	Third Party Pre- Construction, UTSA Post- Construction	SM2540D	
	E. coli (MPN/100 mL)	E. coli	UTSA	IDEXX	
Pesticides and Herbicides	alpha-BHC		Third Party	EPA 3510C	
	Endosulfan I		Third Party	EPA 3510C	
	4,4´-DDE		Third Party	EPA 3510C	
	Dieldrin		Third Party	EPA 3510C	
	Endrin		Third Party	EPA 3510C	

	4,4´-DDD		Third Party	EPA 3510C
	Endosulfan II		Third Party	EPA 3510C
	4,4´-DDT		Third Party	EPA 3510C
	Endrin Aldehyde		Third Party	EPA 3510C
	Endosulfan Sulfate		Third Party	EPA 3510C
	Methoxychlor		Third Party	EPA 3510C
	gamma-BHC (Lindane)		Third Party	EPA 3510C
	Endrin Ketone		Third Party	EPA 3510C
	Toxaphene		Third Party	EPA 3510C
	beta-BHC		Third Party	EPA 3510C
	delta-BHC		Third Party	EPA 3510C
	Heptachlor		Third Party	EPA 3510C
	Aldrin		Third Party	EPA 3510C
	Heptachlor Epoxide		Third Party	EPA 3510C
	gamma-Chlordane		Third Party	EPA 3510C
	alpha-Chlordane		Third Party	EPA 3510C
Total Petroleum Hydrocarbons	C6-C12 Hydrocarbons (mg/L)	TPH	Third Party	TX-1005L
	>C12-C28 Hydrocarbons (mg/L)		Third Party	TX-1005L
	>C28-C35 Hydrocarbons (mg/L)		Third Party	TX-1005L
	Total C6-C35 Hydrocarbons (mg/L)		Third Party	TX-1005L
Fats, Oils, and Greases	Oil & Grease (HEM) (mg/L)	FOG	Third Party	EPA 1664A

Bioretention Basin Effectiveness Data Analysis Approach

To assess the effectiveness of the bioretention basin in retaining water and mitigating downstream peakflows, we compared hydrographs of downstream discharge from the basin to downstream discharge that would have occurred in the absence of the basin. To assess the water treatment effectiveness of the bioretention basin we compared input samples to output samples in the post-construction basin. We also compared the water treatment effectiveness of the basin to the effectiveness measured pre-construction in the grassy channel. We compared the first-flush concentrations, event mean concentrations, and total loads of the input or upstream samples to outlet or downstream samples. We considered one event to be a replicate for statistical analysis purposes.

Hydrograph comparisons

To assess effectiveness of the bioretention basin in mitigating downstream peakflows, we constructed and compared hydrographs with and without the basin installed. Flow level changes in the north and south basin were used to construct both hydrographs. During a storm event, water flowed into the basins and increased the depth of water in the basins up to a maximum depth, which indicated the point at which basins stopped filling. We used the period of increasing depth in the basins to construct the hydrograph that would have occurred in the channel if the basins were not present. The hydrograph was constructed by converting the rate of depth increase to rate of volume increase using known basin geometry (Figure 11), and plotting the change in volume over time (Figure 12). We used the period of decreasing depth in the basins during a storm event to construct the hydrograph that occurred with the basins present. The hydrograph was constructed by converting the rate of depth decrease to rate of volume decrease and plotting the absolute value of change in volume over time (Figure 12). To account for discharge from the basins prior to maximum flow depth, we included a steady rate of discharge, using the average rate of discharge from the declining depth period. Total changes in flow volume for the entire basin were calculated by summing volume changes in the north and south basin. In events with multiple periods of increasing and decreasing depth, we followed the same procedures, using increasing depth for flow without basins and decreasing depth for flow with basins present.

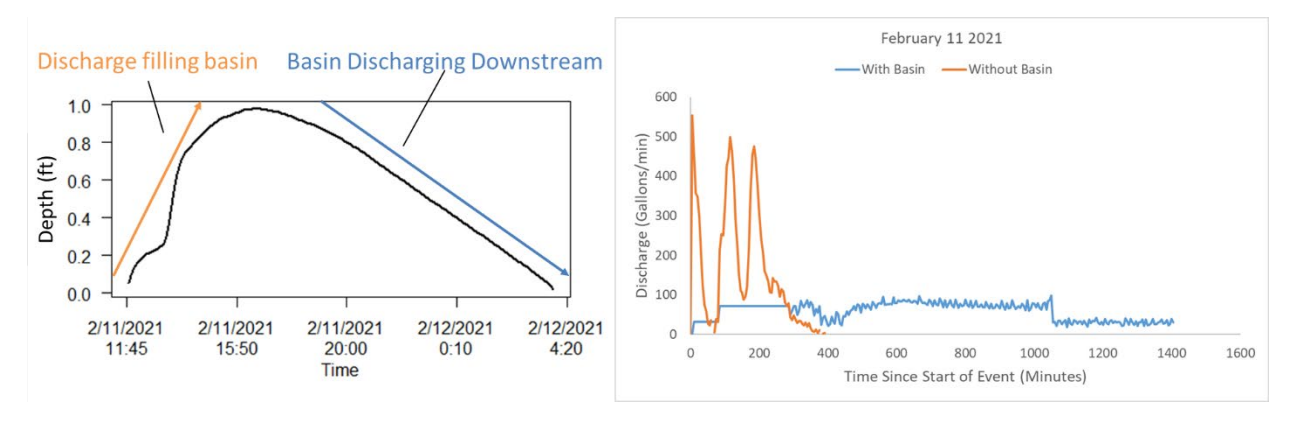


Figure 12. Example showing how water depth changes during a storm event in the bioretention basin were converted to hydrographs with and without the basin present. The left panel shows the recorded water depth in the north basin during an event on 11-12 February 2021. The rate of increase in depth is converted to a rate of volume change, or flow, that would have discharged downstream without the basin present, shown in the orange curve on the right panel. The rate of decrease in depth is converted to a rate of volume change, or flow, that was actually discharged with the basin present, shown in the blue curve on the right panel. The blue curve also includes an average discharge for the period prior to maximum depth. Note the hydrograph does not exactly match the pattern of depth changes in the north basin, because the hydrograph also includes depth changes from the south basin.

First flush concentrations

We compared concentrations of analytes from the first-flush aliquots, which were generally the samples with the highest concentrations of analytes. To test whether analytes were statistically different between the input or upstream first flush aliquots and the outlet or downstream first flush aliquots, we used paired tests in which inlet to outlet or upstream to downstream aliquots were paired for each event. In cases where analytes met assumptions of normality, we used a Student's t-test for paired comparisons. However, many analytes violated normality assumptions, and in these cases a paired Wicoxon rank-sum test was performed. For those analytes where there was a significant reduction in concentration, we calculated mean treatment efficiency by averaging the treatment efficiency for each storm event. Treatment efficiency was calculated using:

$$\left(\frac{input\ or\ upstream\ concentration-outlet\ or\ downstream\ concentration}{input\ or\ upstream\ concentration}
ight)*100$$

To evaluate treatment efficiency for first flush aliquots in the post-construction sampling, we used all events in which at least one basin was sampled and was matched with either an autosampler-collected sump sample or a manually-collected sump grab sample. We considered sump grab samples comparable to first flush aliquots from the basins, because flow-level monitoring in the sump showed a nearly continuous collection and pumping of water from the sump, such that a "first flush" signal was rarely evident inside the sump (Figure 13). In addition, for sump aliquots collected by the autosampler, the first flush concentrations did not differ significantly from any follow-on aliquots, suggesting concentrations remained relatively constant in the sump following storm events. In most events where sump grab samples were collected, only one grab sample was collected, but for the two events in which two sump grab samples were collected, we averaged the concentrations from the two grab samples as the outlet first flush concentration. When only one basin was sampled, we used the concentration from that basin as the input concentration. When both basins were sampled, we compared both the North basin concentrations to the sump and the South basin concentrations to the sump.

Evaluating changes in first flush concentrations in the pre-construction grassy channel required sample collections closely matched in time at both the upstream (site A) and downstream (site B) site. Any first flush aliquots that were considerably out of sync between sites (> 15 minutes) were excluded, yielding between eight and 12 events for first flush comparisons, depending on the analyte.

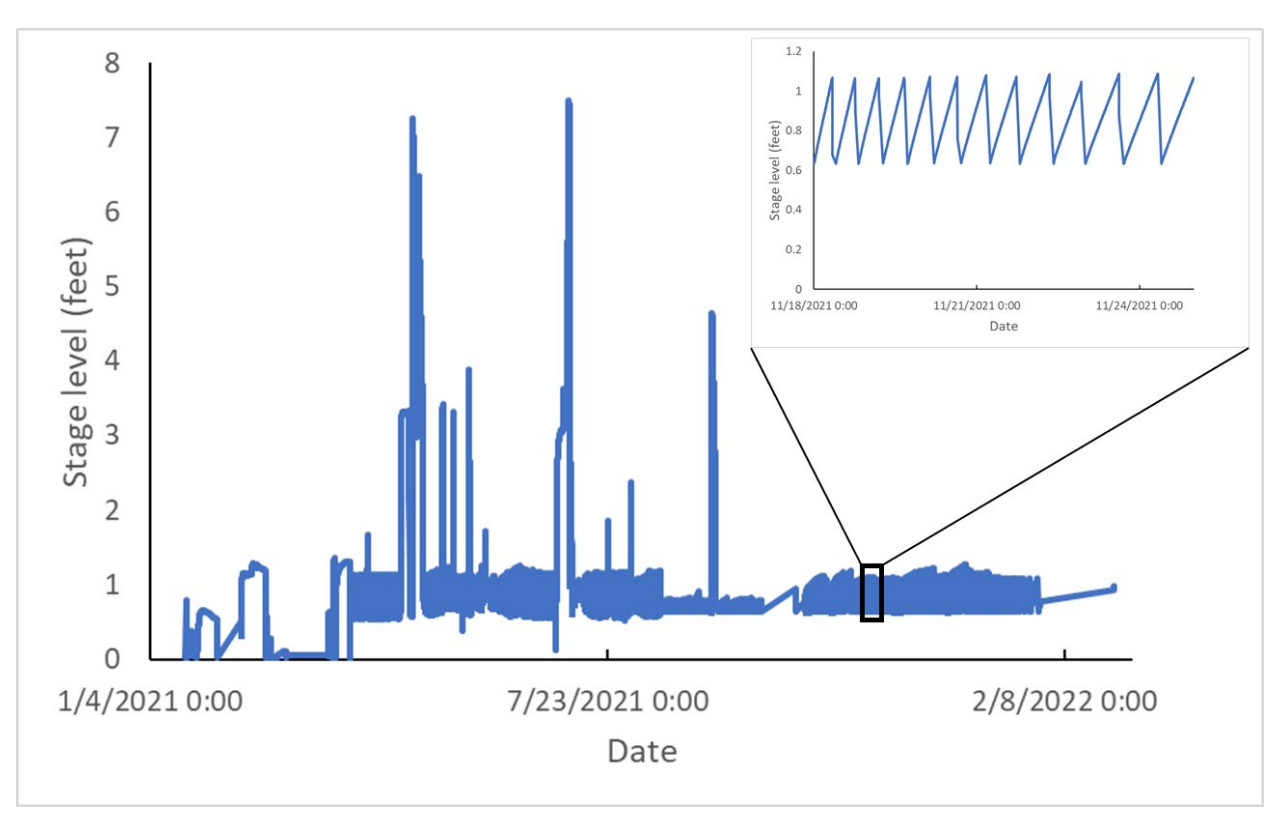


Figure 13. Water level variation in the sump. Inset graph shows normal operation of the sump pump over a period of six days in November 2021, wherein stage level increases as water flows through the underpiping into the sump housing, which turns on the pump and water is pumped out of the sump to draw the water level down. Note that there was a near continuous oscillation of the water level throughout much of the period of monitoring, which made it difficult to attribute water to a specific storm event.

Event mean concentrations

Event mean concentrations were also compared in input or upstream samples to outlet or downstream samples. Event mean concentrations were calculated for the pre-construction sampling sites as the weighted average of aliquots collected across the flow event, with weights determined as the proportion of the total flow volume that passed through the channel between aliquots or the end of the event. For the post-construction sampling we used the aliquot collected closest to the time of peak volume in each basin as the event mean concentration for that basin. We used this approach for event mean concentration because the samples were taken from the comingled and ponded runoff in the basins rather than a flowing channel, such that traditional flow-weighted averaging was not possible. We viewed the sample at the time of maximum ponding depth an appropriate representation of the flow-weighted average, because all the water from the runoff event was comingled in the basin at that time. The event mean concentration for the sump outlet was determined as the same aliquot used for the inlet concentration when the autosampler collected the sump outlet aliquots and otherwise the average of all manual grab samples collected after the storm event. To test whether event mean concentrations were statistically different between the input or upstream samples and the outlet or downstream samples, we used a paired Student's t-test in which inlet to outlet or upstream to downstream samples were paired for each event, unless assumptions of normality and homogeneity of variances were not met, in which case paired Wicoxon ranksum tests were performed. We also calculated mean treatment efficiency for event mean samples that showed significant reductions inlet to outlet or upstream to downstream, using the same approach as for first flush samples.

Total loads

In the pre-construction channel, total loads were calculated by multiplying event mean concentrations by the total volume of the flow event. In the post-construction sampling, total loads for the input were calculated by multiplying the event mean by the maximum volume for each basin separately, and then summing loads from the north and south basin. Due to the near continuous collecting and pumping of water in the sump outlet (Figure 13), it was not possible to determine output volume for a particular event from the sump water level record. We instead assumed that the total input volume was the same as the sump outlet volume for a given event. Given that the output volume was likely somewhat lower than input volume due to evapotranspiration and soil retention, the calculated output loads are likely overestimated, making the estimation of load reductions conservative.

To test whether pollutant loads were statistically different between the input or upstream samples and the outlet or downstream samples, we used a paired Student's t-test in which inlet to outlet or upstream to downstream samples were paired for each event, unless assumptions of normality and homogeneity of variances were not met, in which case paired Wilcoxon rank-sum tests were performed.

Reliable calculation of flow volumes in the pre-construction grassy channel was restricted to flow events that came to a natural end within the collection capacity of the autosamplers. For example, if an autosampler had collected the maximum capacity of four flushes and the event continued for more than one designated flow pulse (about 15 minutes of flow in a half-full channel), the event was excluded from event mean and total load comparisons due to the unknown concentrations at the latter end of the flow event. Only events where both samplers met this condition were included. This yielded between four and six matched pairs for evaluation of the pre-construction channel, depending on the analyte. In the post-construction sampling, there were a minimum of three and maximum of 10 matched storm events for evaluation, depending on the analyte.

Temperature spikes

In analyzing temperature data, we focused on temperature spikes in stormwater that occurred when rainfall absorbed heat from ground surfaces. We calculated the difference between maximum water temperature during a storm event and air temperature just prior to runoff (Figure 14). Maximum water temperature usually occurred within the first 5-10 minutes of the start of a runoff event. The initial goal was to determine whether temperature spikes were muted in the sump outlet water compared to spikes observed in the basins and in the preconstruction channel. Unfortunately, due to a combination of delayed data retrieval and temperature logger malfunctioning, no temperature data was recorded in the sump outlet during the study period. Instead, we focus on temperature changes over time in the basins during runoff events.

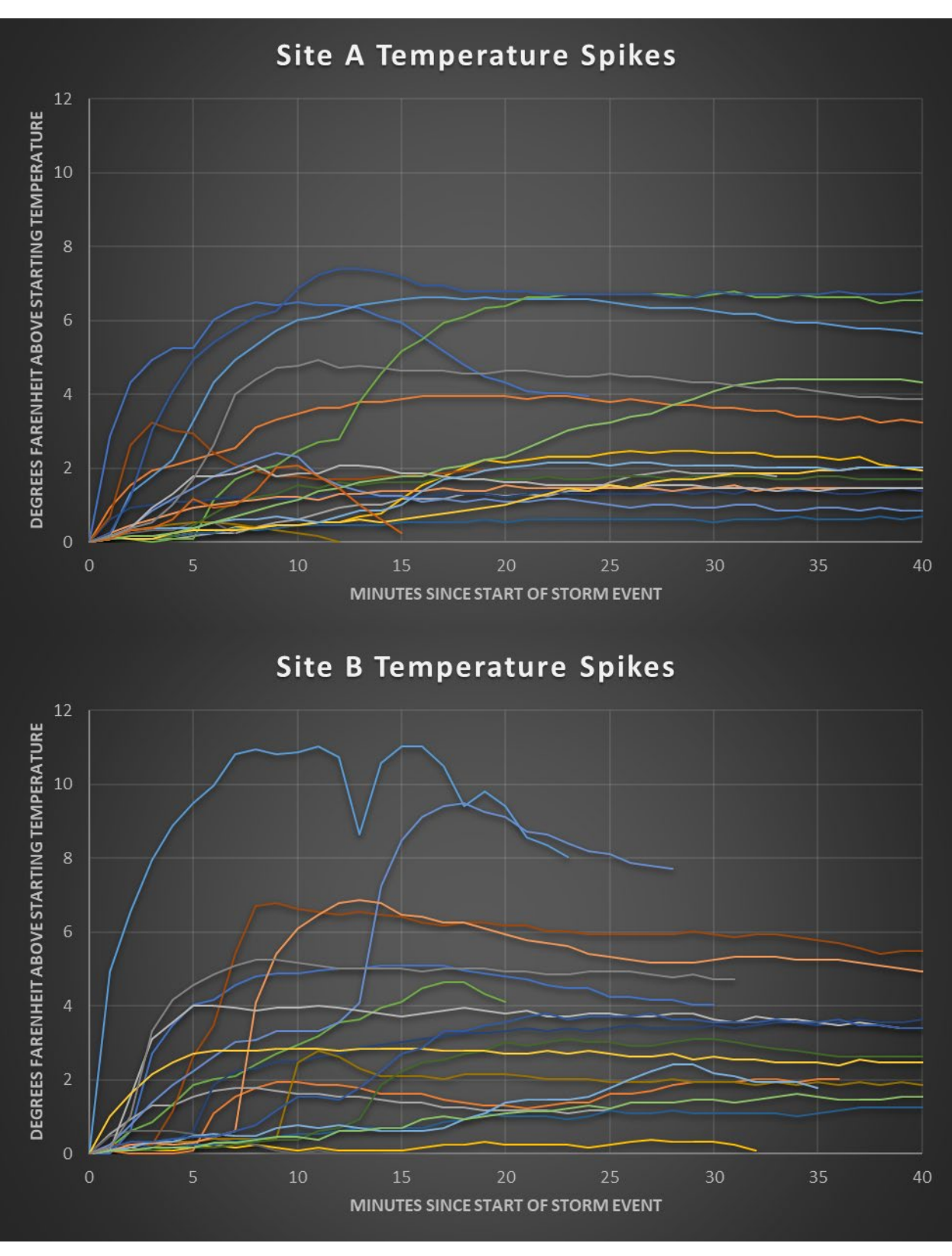


Figure 14. Plots showing temperature spikes from all recorded runoff events in the preconstruction upstream (site A) and downstream channels (site B).

Current Operation of LID Facilities

Construction and installation of all LID facilities was completed in November 2020. Two years after construction completion, all facilities are operating as designed from a hydrological and aesthetic standpoint. The cisterns capture water from two building rooftops during storm events and the water stored is connected to the grey water piping system on the campus for irrigation purposes. Water ponds in both basins of the bioretention basin during storm events, and the water effectively drains through the biomedia fill over a period of at most several days. The sump pump is operating to remove water out of the basins, though there were some issues early post-construction with the floats operating the pump automatically.

The LID facilities are also providing educational and aesthetic benefits to the campus community and visitors to campus. Informational signs are installed at each LID facility (Figure 8). There are also chairs, lights, and a charging station near the bioretention basin, which provide outdoor studying, gathering, or relaxing space (chairs can be seen Figure 8). There is a footpath along the bioswale and unmowed grassy channel which is heavily trafficked by students walking from a commuter parking lot to university buildings. Some planted vegetation at the bioretention basin and bioswale was lost due to drying, deer rubbing, and a hard freeze that occurred soon after project completion. However, despite some losses, the planted vegetation around the bioretention basin and bioswale has also grown in well, providing an aesthetically pleasing environment, especially when the basins are filled with water (Figure 15).

Maintenance activities are primarily focused on maintaining the aesthetic environment of the bioretention basin. Student volunteers participate in bioretention basin cleanups two to three times a semester, with activities primarily focused on weeding vegetation and picking up trash in and around the bioretention basin. The facilities department of UTSA also uses trimmers to cut back weedy vegetation periodically, on average two to three times a year.

Bioretention Basin Effectiveness Study Results

Flow Attenuation

Comparison of estimated hydrographs with and without the bioretention basin present indicated the bioretention basin system effectively attenuated peak flow level downstream during runoff events (Figure 16). Flow events without the basin present typically lasted between two and seven hours with peakflows typically between 500-5000 gallons/minute. Flow events with the basin present typically lasted several days with peakflows of 90-200 gallons/minute. Thus, instead of flow being conveyed immediately downstream, a large amount of runoff is stored, filtered, and released downstream at a much slower rate with the bioretention basin present. Flow patterns in the grassy channel prior to construction showed similar patterns to the estimated flows without the basin, with rapid increases in flow rate to peakflow followed by declines back to zero flow over several hours. All flow pumped out of the basins is further attenuated and treated by the unmowed grassy channel and bioswale.

However, it is important to note the bioretention basins have a maximum capacity, such that any storm events that exceed this capacity will not be effectively attenuated. Flow monitoring indicated there were four storm events that did exceed basin capacity over the period February 2021 to February 2022.



Figure 15. Photographs show growth of planted vegetation in the bioretention basin over time. The left photo was taken two months after basin construction, the right photo was taken almost two years after basin construction.

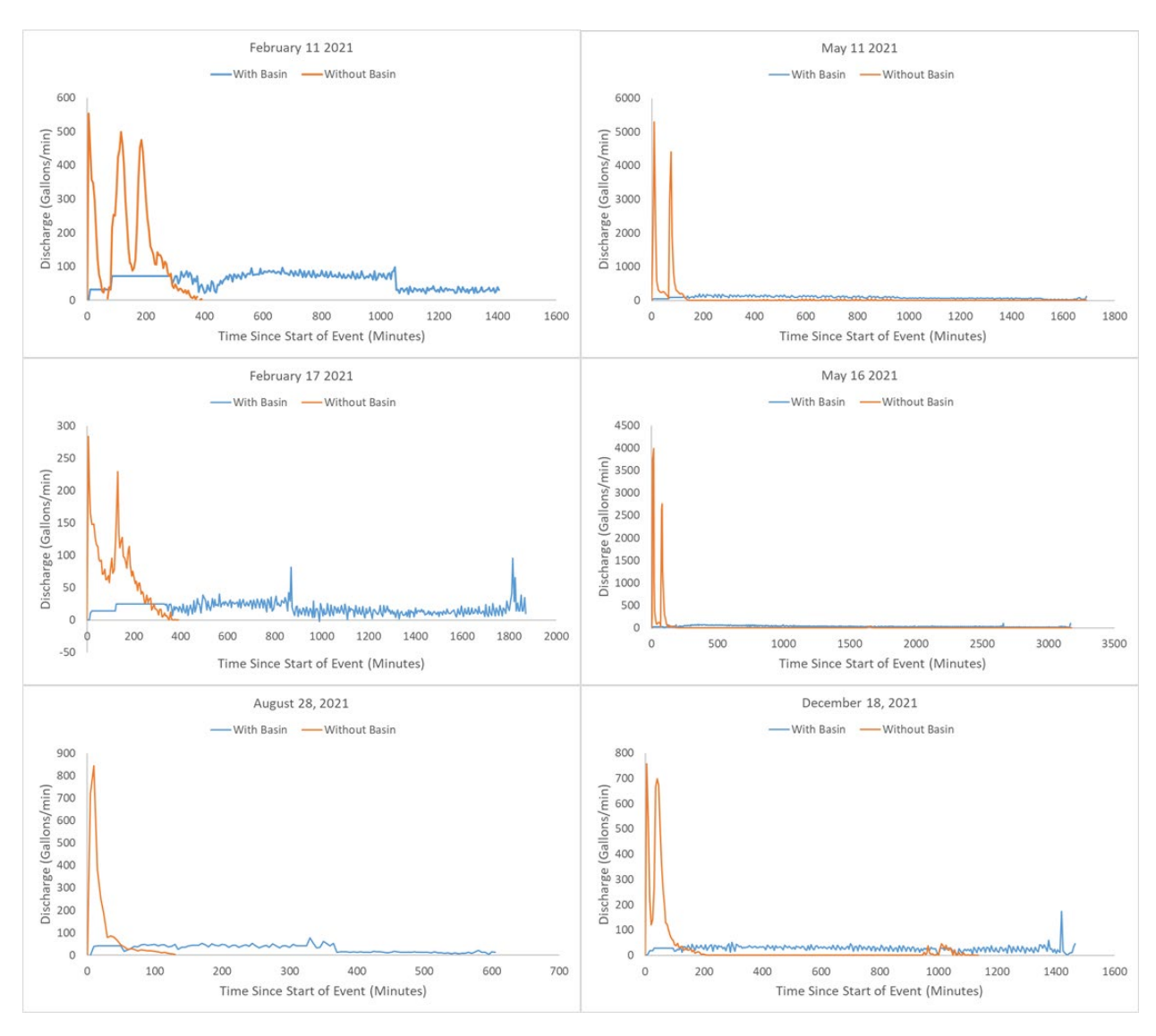


Figure 16. Hydrographs comparing the flow released from the bioretention basin to estimated flow that would have occurred without the basin. Each panel is a different storm event.

Pre-Construction Water Quality Sampling Summary

The autosampler/flow meter arrays and temperature loggers were installed in mid-June 2018. The first grab samples were collected on 4 July 2018 and the first flow event collected by autosamplers occurred on 10 August 2018 (Table 2). Manual grab samples from HEB SU and Convocation outfalls were added to the sampling plan on 15 October 2018. These were not always collected due to the need for personnel to be on site as the flow event was beginning. The last flow event collected in the pre-construction phase occurred on 9 June 2019. All sampling was suspended after 11 October 2019 with the start of bioretention basin construction.

A total of 17 flow events were sampled in the pre-construction phase. Within a given flow event, between one and ten samples were collected, depending on the length of the flow event, the number of flushes collected by autosamplers at sites A and B, and whether grab samples from the outfalls were collected. Although most analytes were measured for all successful sampling events, some exceptions included lack of nitrate (NO_3^-), total phosphorus (TP), and metals for the last several collection events due to having already collected the funding agreement-required five events and needing to ensure sufficient funding for post-construction sampling (Table 3). As such, n-values for each analyte were different from the number of flow events collected.

Total flow volumes for events that were used in load calculations ranged from 133-24,276 gallons at the upstream sampling point (site A) and 1,243 to 11,526 gallons at the downstream sampling point (site B). In all but one storm event, there was greater flow at the downstream sampling site due to the addition of runoff from sections of the campus, including the HEB SU and Convocation rooftops. Values of specific conductance (SC), total dissolved solids (TDS), total suspended solids (TSS), total nitrogen (TN), and TP were within ranges found in stormwater runoff in other urban areas throughout the U.S. (Pitt, Maestre, & Morquecho, 2004). The mean pH of runoff was somewhat more basic than neutral and ranged from 7.25 to 9.79 (Table 4).

Pesticides, herbicides, and total petroleum hydrocarbons (TPH) were analyzed from all collected aliquots at both sites A and B for events on 10 August, 3 September, 26 September, 30 September, and 8 October 2018. Multiple compounds were tested for (see Table 1), but no pesticides, herbicides or TPH compounds were detected. Thus, neither pesticides and herbicides nor TPH were tested in further samples.

Grab samples for fats, oils and greases (FOG) were also collected when personnel were onsite during events on 4 July, 10 August, 3 September, 8 October, and 31 October 2018 and 11 January 2019. A FOG concentration of 10 mg/L was found at site A from the event on 4 July, but no other samples from sites A or B yielded detectable concentrations, and further samples for FOG were not collected. Samples collected between 10 August 2018 and 13 April 2019 were run for multiple metals. Silver, arsenic, cadmium, chromium, and selenium were never detected. Lead and mercury were detected only once each, during the first flush from events 8 October

2018 and 10 August 2018, respectively. Further analysis and discussion of metals thus focuses only on barium, copper, and zinc.

Table 2. Summary of successful collection events in the pre-construction monitoring phase.

Event	A 1st	A FO 1	A FO 2	A FO 3	B 1st	B FO 1	B FO 2	B FO 3	HEB SU	Convo
7/4/2018	< M	achine program	collected too qu	ickly>	< Machine	e program did no	t collect sufficie	ent quantity >		
8/10/2018	✓	program end	×	×	✓	program end	×	×		
9/3/2018	✓	~	*	*	✓	~	program end	×	Samples from thes	
9/22/2018	✓	✓	program end	×	<	Machine fa	iled to initiate	>	sites w	ere not
9/26/2018	✓	~	~	program end	✓	✓	program end	×		until after
9/30/2018	✓	✓	✓	program end	✓	program end	×	×	10/15	/2018
10/8/2018	✓	~	~	✓	✓	program end	×	×		
10/15/2018	<	Machine fai	led to initiate	>	no start	✓	program end	×		
10/31/2018	✓	✓	~	✓	✓	✓	✓	✓	~	
11/8/2018	✓	**	~	✓	✓	✓	✓	✓	D1	
12/7/2018	✓	✓	✓	✓	✓	program end	×	×	Personnel not on sit at event start	
12/26/2018	✓	✓	✓	**	✓	✓	✓	✓		
1/11/2019	✓	✓	✓	✓	✓	✓	✓	✓	✓	~
1/22/1900	✓	~	✓	✓	✓	✓	✓	program end		
1/27/2019	✓	✓	✓	✓	✓	✓	✓	✓	D 1	
3/13/2019	✓	~	~	✓	✓	✓	✓	✓		not on site
4/13/2019	no start	✓	✓	✓	✓	✓	✓	✓	at eve	ii start
5/30/2019	✓	✓	program end	×	✓	✓	✓	program end		
6/4/2019	✓	✓	✓	program end	✓	✓	✓	✓	✓	✓
6/9/2019	✓	✓	✓	✓	✓	✓	✓	✓	✓	~
9/19/2019	✓	✓	✓	✓	✓	✓	✓	✓	Personnel	not on site
10/11/2019	✓	✓	✓	program end	✓	✓	✓	✓	at ever	nt start

Notes: "A" and "B" denote the autosampler site. "1st" denotes first flush while "FO" denotes the subsequent flow-paced collections with the corresponding number denoting the sequence. "\$" denotes that the sample was discarded due to confusion on collection protocol, while "**" denotes that the sample was mistakenly discarded before being sent to SATL. Check marks denote successful collections while "×" denotes collections not obtained following the completion of a normal program.

Table 3. Summary of analytes measured for each collection event in the pre-construction monitoring phase.

Event	рН	SC	TDS	TSS	Nutrients (except TP)	TP	Metals	Pesticides and Herbicides	TPH	FOG
7/4/2018					,			11010101000		~
8/10/2018				✓	✓		✓	~	✓	/
9/3/2018				✓	✓		✓	✓	✓	✓
9/22/2018	✓	✓	✓	✓	✓	✓	✓	✓	✓	
9/26/2018	✓	✓	✓	✓	✓	✓	✓	✓	✓	
9/30/2018	✓	✓	✓	✓	✓	✓	✓	✓	/	
10/8/2018	✓	✓	✓	✓	✓	✓	✓	✓	✓	✓
10/15/2018	✓	✓	✓	✓	✓	✓	✓			
10/31/2018	✓	✓	✓	✓	✓	✓	~			~
11/8/2018	✓	✓	✓	✓	✓	✓	✓			
12/7/2018	✓	✓	✓	✓	✓	✓	~			
12/26/2018	✓	✓	✓	✓	✓	✓	~			
1/11/2019	✓	✓	✓	✓	✓	✓	✓			✓
1/22/2019	✓	✓	✓	✓	✓	✓	~			
1/27/2019	✓	✓	✓	✓	✓	✓	~			
3/13/2019	✓	✓	✓	✓	✓	✓	✓			
4/13/2019	✓	✓	✓	✓	✓	✓	✓			
5/30/2019	✓	✓	✓							
6/4/2019	✓	✓	✓							
6/9/2019	✓	✓	✓							

Table 4. Summary of average concentrations and ranges for analytes measured during the preconstruction phase across all sample sites. Units are μ S/cm for SC, pH units for pH and mg/L for all others. Samples with non-detections for individual analytes were excluded from calculations.

Variable	n	Min	Max	Mean	Median		sd
рН	107	7.25	9.79	8.54	8.47	±	0.63
SC	111	17.2	758	117	95.4	±	102
TDS	111	23.0	493	75.9	62.0	±	66.1
TN	91	0.00	16.4	1.37	1.04	±	2.02
NO ⁻ 3	91	0.13	3.02	0.61	0.50	±	0.46
TP	85	0.00	3.31	0.23	0.15	±	0.40
TOC	91	1.56	164	12.5	7.48	±	20.1
TSS	91	0.00	386	44.6	15.0	±	75.1
Barium	59	0.01	0.09	0.02	0.02	±	0.02
Copper	50	0.01	0.31	0.03	0.02	±	0.05
Zinc	96	0.01	0.22	0.04	0.03	±	0.04

Treatment efficiency in the pre-construction grassy channel

Mean first flush pH and TSS concentrations significantly decreased as stormflows moved through the channel from site A to site B; median first flush concentrations of SC, TDS, and TOC increased from upstream to downstream (Table 5; Figure 17). No significant differences were observed between sites A and B for first flush concentrations of TN or TP. Copper was higher in first flush concentrations at the downstream site (site B) compared to the upstream site (site A) and zinc was higher at the upstream site compared to the downstream site (Figure 17). Using events which showed a decrease from upstream to downstream, mean treatment efficiencies for analytes that significantly decreased were 72% for TSS and 45% for zinc.

Table 5. Paired test results for changes in first flush concentrations from upstream to downstream in the pre-construction grassy channel.

Analyte	Test type	Test statistic	Direction of change (if significant)	p-value
рН	t-test	6.784	Decrease	<0.0001
SC	Signed-rank	0.000	Increase	0.0005
TDS	Signed-rank	0.000	Increase	0.0025
TN	Signed-rank	19.000	None	0.9442
NO ⁻ 3	Signed-rank	30.000	None	0.8240
TP	t-test	0.774	None	0.4610
TOC	Signed-rank	9.000	Increase	0.0322
TSS	t-test	3.093	Decrease	0.0114
Barium	Signed-rank	21.000	None	0.7422
Copper	Signed-rank	8.000	Increase	0.0488
Zinc	Signed-rank	74.000	Decrease	0.0479

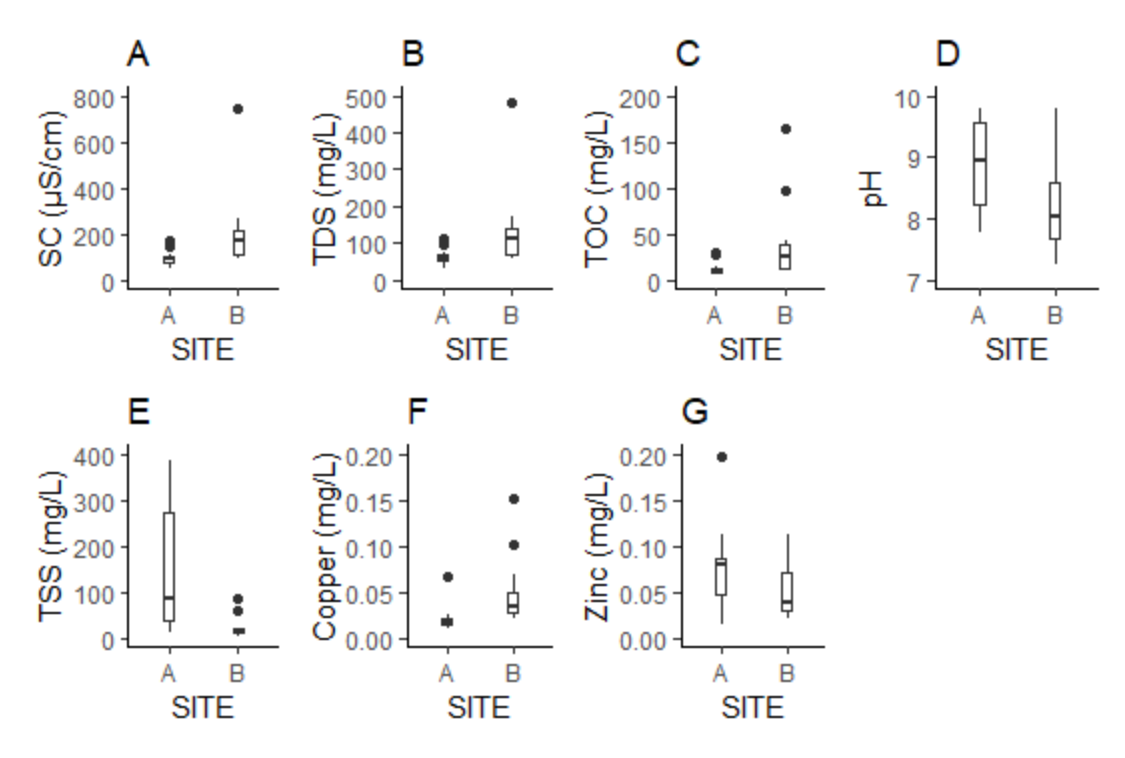


Figure 17. Distributions of analyte first-flush concentrations that showed significant changes from upstream to downstream in the pre-construction grassy channel. Measures of A) specific conductance (SC), B) total dissolved solids (TDS), C) total organic carbon (TOC), and F) copper increased from upstream to downstream. Measures of D) pH, E) total suspended solids (TSS), and G) zinc decreased.

The only analyte that changed significantly in total load from upstream to downstream in the pre-construction channel was TDS, which increased significantly (Table 6), due to a combination of event mean concentration and total flow being higher on average in the downstream sampling site (Table 7). The mean TDS load increased from 0.2 kg per event at the upstream site to 4.2 kg per event at the downstream site. The event mean concentration of TOC was also significantly higher at the downstream site, but this did not translate to a significant increase in total load (Tables 6 and 7). The total load for TOC across both sites averaged 0.3 kg per event. The total load per event for TSS was 0.5 kg and for TN and TP was 0.05 kg and 0.003 kg, respectively. Mean loads of metals were 0.2 g, 0.4 g, and 0.7 g for barium, copper, and zinc respectively. No significant changes were observed in event mean concentrations or loads between sites A and B for any other parameters tested (Tables 6 and 7).

Table 6. Paired test results for upstream to downstream differences in flow event loads in the pre-construction channel.

Analyte	Test type	Test statistic	Direction of change (if significant)	p-value
TDS	Signed-rank	0.000	Increase	0.0313
N	Signed-rank	3.000	None	1.0000
NO ⁻ 3	Signed-rank	1.000	None	0.1250
TP	t-test	-2.105	None	0.1230
TOC	Signed-rank	2.000	None	0.1875
TSS	Signed-rank	9.000	None	0.8125
Barium	Signed-rank	0.000	None	0.5000
Copper	Signed-Rank	2.000	None	0.1875
Zinc	t-test	5.000	None	0.6250

Table 7. Paired test results for upstream to downstream differences in event means in the preconstruction channel.

Analyte	Test type	Test statistic	Direction of	p-value
			change (if	
			significant)	
TDS	Signed-Rank	0.000	Increase	0.0313
N	Signed-Rank	2.000	None	0.3613
NO ⁻ 3	Signed-Rank	0.000	None	0.0625
Р	t-test	-0.349	None	0.7503
TOC	t-test	-6.366	Increase	0.0031
TSS	Signed-Rank	14.000	None	0.1250
Barium	t-test	8.149	None	0.0774
Copper	Signed-Rank	0.000	None	0.0625
Zinc	t-test	-0.347	None	0.7460

Pre-construction temperature

Temperature at both sites and A and B was recorded for all events except 7 December 2018. Ground temperatures routinely exceeded 100 F in the summer months, which caused noticeable temperature increases in stormwater runoff for nearly all runoff events monitored. Even in winter, runoff events routinely showed noticeable temperature spikes, although maximum water temperatures were lower compared to summer runoff events. Temperature spikes averaged approximately 3.5 F across both sites (Figure 18), with a maximum of 9.7 F.

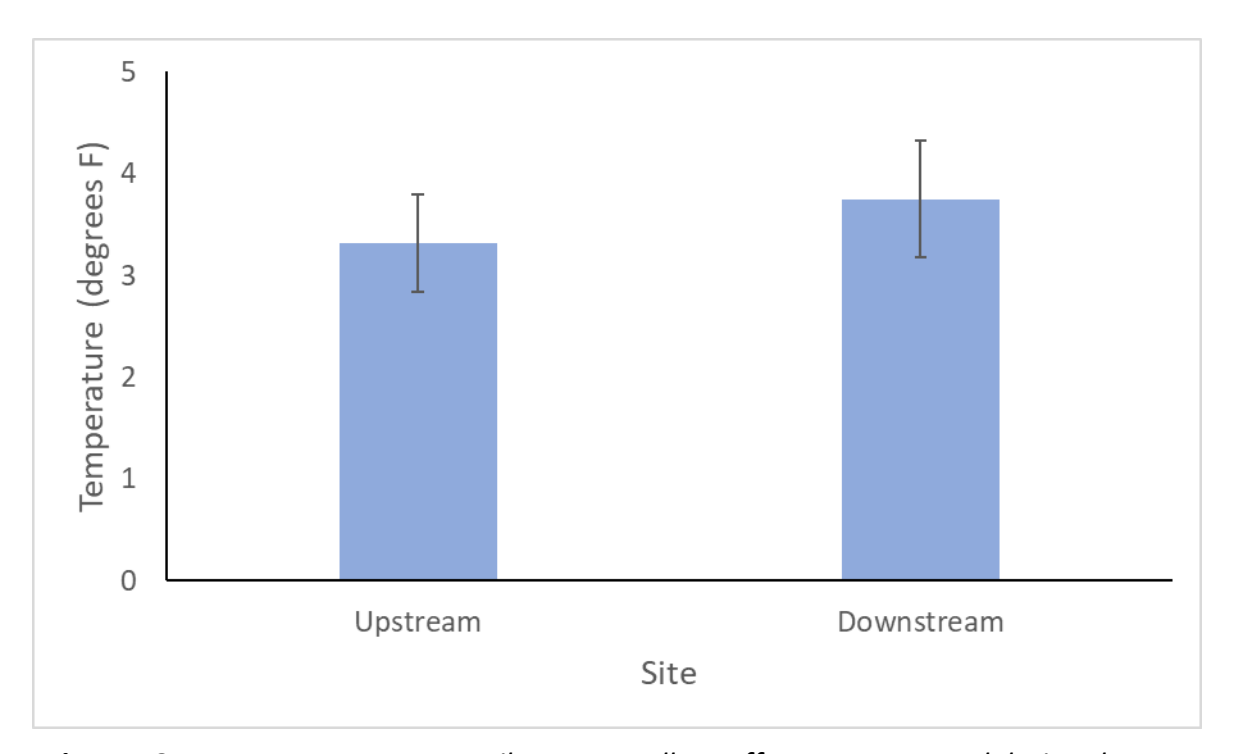


Figure 18. Average temperature spikes across all runoff events measured during the preconstruction phase in both the upstream (site A) and downstream (site B) sites. Temperature spikes are defined as the difference between maximum water temperature and ambient air temperature at the start of the runoff event. Error bars are standard errors.

Post-Construction Water Quality Sampling Summary

Construction of the bioretention basin was completed in November 2020. The autosampler/flow meter arrays and temperature loggers were installed in January 2021. The first storm event collected by autosamplers at the north and south basins occurred on 12 February 2021 (Table 8). Due to malfunctioning of loggers, temperature data was not available

for events prior to 14 October 2021 except for the north basin. The last storm event collected in the post-construction monitoring phase occurred on 3 February 2022.

A total of 15 storm events were sampled in the post-construction phase. Samples from both the north and south basins were collected for most storm events, but four events had only one basin sampled (Table 8). In most storm events, the autosamplers in the basins collected four aliquots, corresponding to a first flush and three follow-on aliquots spaced one hour apart. When autosamplers sampled the sump outlet, four aliquots were collected for all but one event. When the sump outlet was sampled by manual grab sampling, at most two aliquots were collected, spaced an hour apart. No analytes had matched basin and sump samples for all 15 events, but all analytes except TP had more than five matched samples (Table 8).

Estimated total flow volumes for events that were used in load calculations for the post-construction sampling ranged from 23,197 to 500,850 gallons, with a range of 4,784 to 126,992 gallons in the north basin and 18,414 to 373,858 gallons in the south basin. First flush concentrations of most analytes in the basin inlet were generally similar to pre-construction concentrations, though TN was somewhat lower in the basin inlet samples (Table 9). Event mean concentrations were also generally similar for most analytes in the basin inlet samples compared to pre-construction samples, with notable exceptions for TDS and TP, which were generally lower post-construction, and TSS, which was generally higher post-construction (Table 10). Due to uncertainty in flow volume estimates in both the pre and post-construction monitoring periods, direct comparison of loads between pre and post-construction periods was not done. Instead, comparisons were made of the changes in loads upstream to downstream and basin input to basin outlet.

Total petroleum hydrocarbons (TPH) were analyzed from all collected samples for events on 12 February, 23 March, 23 April, 29 April, 16 May, and 23 May 2021. No TPH were detected in any samples. Pesticides and herbicides were not analyzed in post-construction samples.

Statistical analysis of metals for the post-construction sampling focused on barium, copper, and zinc, as in the pre-construction sampling, but also included arsenic, which was detected in the sump outlet during six events and in the south basin during two events. Barium was detected in six matched events and zinc was detected in seven matched events. Copper was detected in the basin samples during six events, but only during one event in the sump outlet. Thus, due to having only one matched event for arsenic and copper, statistical analysis was possible only for barium and zinc. Chromium was never detected in post-construction sampling. Cadmium was detected only once, in the south basin, with a concentration at the detection limit (0.005 mg/L). Lead was detected only twice, once in the north basin and once in the south basin during separate events. Mercury, silver, and selenium were not analyzed in the post-construction sampling.

Table 8. Summary of events sampled in the post-construction monitoring phase, where matched basin and sump samples were available for at least one analyte. A check mark in the analyte column indicates matched basin and sump samples were available for the corresponding event date.

Event	pH, SC,	E. coli	TN	NO ₃ -	NH ₃ -	TP	TOC	Metals*
	TDS,TSS							
2/12/2021	✓	✓				✓	✓	~
3/23/2021	✓		✓				✓	✓
4/23/2021	✓	✓	✓	✓			✓	✓
4/29/2021	✓	✓	✓	✓			✓	✓
5/12/2021	✓	✓	✓	✓				✓
5/16/2021	✓	✓		✓			✓	✓
5/23/2021	✓	✓		✓			✓	✓
9/5/2021	✓							✓
9/29/2021	✓	✓	✓		✓			
10/11/2021	✓	✓	✓		✓	✓		
10/14/2021	✓		✓	✓	✓			
10/27/2021			✓	✓	✓	✓		
11/4/2021	✓		✓	✓	✓			
12/17/2021			✓		✓			
2/3/2022			✓	✓	✓	✓		

^{*}Due to concentrations below detection limits, not all events had matched pairs available for statistical analysis for all metals

Table 9. Mean ± standard errors for first flush concentrations for selected analytes in the upstream (site A) and downstream (site B) sites in the pre-construction channel and the north (NB) and south basins (SB) and the sump outlet (Sump) in the post-construction bioretention system. Sump outlet values include grab samples. Ba = barium; Cu = copper, Zn = zinc; As = arsenic. All units are mg/L except E. coli, which is MPN/100mL. ND = non-detection, blank entry = not measured.

Site	TDS	TSS	TOC	TN	NO ⁻ 3	TP	Ва	Cu	Zn	As	E. coli
Site A	64.1	144	11.7	3.8	0.5	0.3	0.03	0.02	0.08	ND	
	±	±	±	±	±	±	±	±	±		
	6.1	40.6	2.3	1.7	0.09	0.06	0.007	0.005	0.01		
Site B	142.5	21	42.3	3.2	0.8	0.2	0.02	0.05	0.05	ND	
	±	±	±	±	±	±	±	±	±		
	32.4	6.1	12.8	0.9	0.2	0.05	0.01	0.01	0.008		
NB	62.4	123	9.3	1.5	0.6	0.1	0.02	0.02	0.3	ND	13,431
	±	±	±	±	±	±	±	±	±		±
	4.4	32.9	1.1	0.6	0.2	0.03	0.003	0.004	0.3		5,637
SB	73.7	53	16.3	1.0	0.4	0.05	0.02	0.02	0.04	0.01	35,340
	±	±	±	±	±	±	±	±	±	±	±
	10.2	12.0	3.7	0.3	0.1	0.02	0.004	0.002	0.02	0.01	38,559
Sump	401	456	14.4	1.5	0.3	0.08	0.1	0.003	0.5	0.02	1001
	±	±	±	±	±	±	±		±	±	±
	44.5	450	0.1	0.3	0.09	0.06	0.01		0.43	0.003	685

Table 10. Mean \pm standard errors for event mean concentrations in the upstream (site A) and downstream (site B) sites in the pre-construction channel and the north (NB) and south basins (SB) and the sump outlet (Sump) in the post-construction bioretention system. Sump outlet values include grab samples. Ba = barium; Cu = copper, Zn = zinc. All units are mg/L except E. coli, which is MPN/100mL. Blank entry = not measured.

2011, 11111		,		, ,						
Site	TDS	TSS	TOC	TN	NO ⁻ 3	TP	Ва	Cu	Zn	E. coli
Site A	111	65	7.8	1.7	0.1	0.3	0.02	0.02	0.04	
	±	±	±	±	±	±	±	±	±	
	49	32	1.6	0.4	0.04	0.1	0.004	0.01	0.005	
Site B	248	36	28.5	3.7	0.5	0.3	0.01	0.06	0.04	
	±	±	±	±	±	±	±	±	±	
	95	29	4.0	2.6	0.2	0.2	0.005	0.03	0.01	
NB	44.1	544	5.2	1.2	0.3	0.06	0.01	0.01	0.30	11,820
	±	±	±	±	±	±	±	±	±	±
	5.5	538	0.9	0.4	0.09	0.01	0.001	0.002	0.30	5,797
SB	58.4	745	11.0	1.3	0.3	0.07	0.02	0.01	0.03	10,932
	±	±	±	±	±	±	±	±	±	±
	10.8	763	2.0	0.4	0.1	0.02	0.001	0.002	0.009	5,432
Sump	375.7	761	14.7	1.3	0.4	0.11	0.11	0.003	0.52	1,114
	±	±	±	±	±	±	±		±	±
	49.8	684	1.5	0.3	0.06	0.08	0.02		0.51	758

Treatment efficiency in the constructed basin

First flush measurements of pH, nitrate (NO_3^-), total suspended solids (TSS) and E. coli were significantly lower in the sump outlet compared to the north basin inlet samples, but only E. coli was marginally significantly lower in the sump outlet compared to south basin inlet samples (Table 11, Figure 19). Across all events for the north basin, treatment efficiency for NO₃ averaged 57%, for TSS averaged 13%, and for *E. coli* averaged 78%. There was also evidence that copper and TP concentrations were lower in the sump outlet. Copper was tested in seven matched events, and was found in detectable concentrations in six events in the north basin and three events in the south basin, but in only one event at the sump outlet. Total phosphorus was tested in 12 matched events, was found in detectable concentrations in 10 events in the north basin and seven events in the south basin, but in only 4 events in the sump outlet. The lack of detection in the outlet samples precluded statistical testing and treatment efficiency calculation for copper because no events had detectable concentrations in both the basins and the sump outlet, but indicates that copper was usually lower in concentration in the outlet compared to inlet water. The same is true for TP, though TP was not statistically different for the north basin and sample concentrations in the basin inlets were also quite low. In contrast, arsenic was detected in the sump outlet during six events, but was not detected during any events in the north basin and in only two events in the south basin, suggesting there may have been accumulation of arsenic in the water while filtering through the basin sediments. Concentrations of total dissolved solids (TDS) were also higher in the sump outlet compared to both basins and concentrations of barium and total organic carbon (TOC) were higher in the sump outlet compared to the north basin.

Flow events that yielded useable load data showed a mean total load of 40 kg TDS entering the basins, but due to the increased concentrations leaving the basin, the sump outlet had a mean load of 263 kg, which was a statistically significant difference (Table 12). The only other tested analyte which showed a significant difference in load between the basin inlets and sump outlet was *E. coli*, which was reduced in the sump outlet compared to the basins (Table 12). The event mean concentrations for TDS and *E. coli* were significantly different in the sump outlet compared to both the north and south basin inlets, with TDS higher and *E. coli* lower in the sump outlet compared to the basins (Figure 20). The only other analyte that showed a significant difference in event mean concentration between the basins and sump outlet was TOC, which was higher in the sump outlet compared to the north basin. Average treatment efficiency for *E. coli* was 79% for all events in the north basin and 89% for all events in the south basin.

Table 11. Paired test results for North Basin (NB) and South Basin (SB) inputs compared to outlet (Sump) first flush concentrations in the bioretention basin.

Analyte	Test type	Direction of change	NB vs. Sump	SB vs. Sump
		(if significant)	p-value	p-value
рН	Signed-Rank	Decrease	0.02	0.20
SC	Signed-Rank	Increase	0.0005	0.004
TDS	Signed-Rank	Increase	0.0005	0.004
TN	Signed-Rank	None	0.46	0.94
NO ⁻ 3	Signed-Rank	Decrease	0.01	1.00
NH^{+}_{4}	Signed-Rank	None	0.09	0.13
TP	Signed-Rank	None	1.00	-
TOC	t-test	Increase	0.001	0.65
TSS	Signed-Rank	Decrease	0.009	0.11
Barium	Signed-Rank	Increase	0.03	0.25
Copper	Not tested	-	-	-
Zinc	Signed-Rank	None	0.69	1.00
E. coli	Signed-Rank	Decrease	0.008	0.06

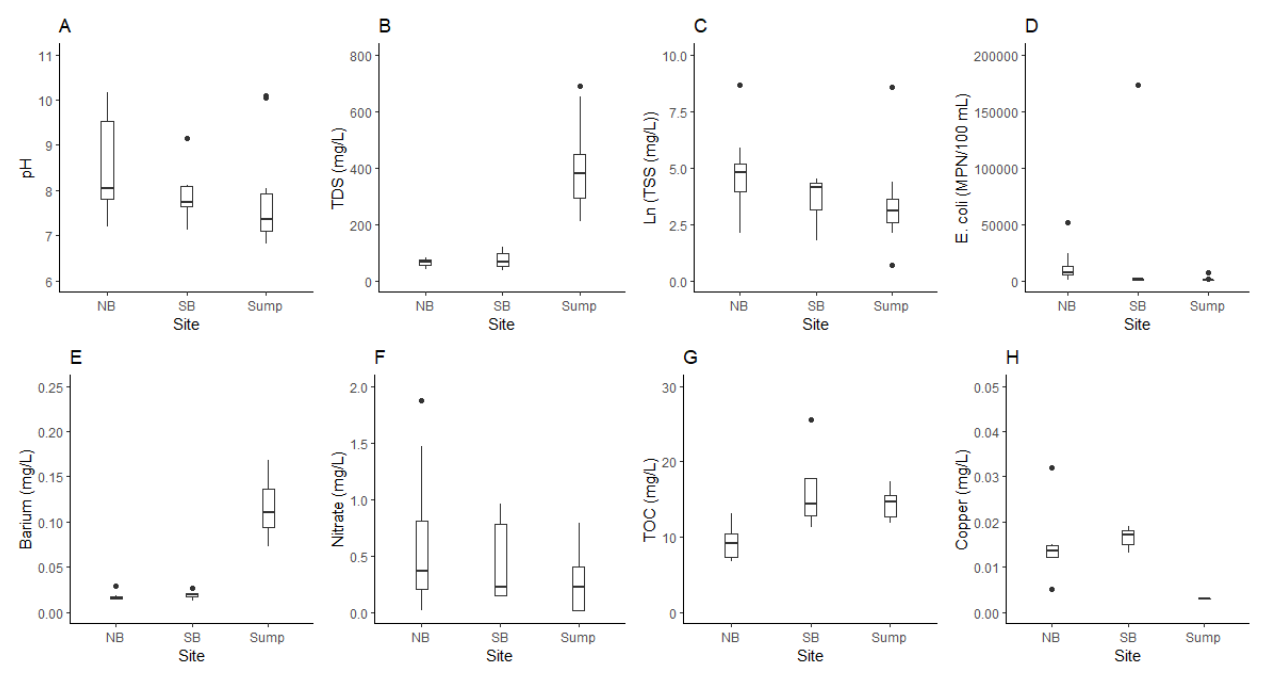


Figure 19. Distributions of analyte first-flush concentrations that showed significant or nearly significant changes from north basin (NB) and south basin (SB) inputs to outlet (Sump) in the bioretention basin. Measures of B) total dissolved solids (TDS), E) barium, and G) total organic carbon (TOC) increased in the sump outlet compared to at least one basin. Measures of A) pH, B) total suspended solids (TSS), D) E. coli, and F) nitrate decreased in the sump outlet compared to at least one basin. Detections of H) copper were less frequent in the sump compared to the basin inlets.

Table 12. Mean loads for selected analytes in the basin and in the basin output. SE = standard error. Those marked with an * are statistically significantly different between the basin and sump outlet.

Analyte	Mean load in	Mean load in		
	basins (kg) ± SE	sump outlet (kg)		
TDS (kg)*	40 ± 10	263 ± 77		
TSS (kg)	184 ± 159	205 ± 164		
TN (kg)	0.95 ± 0.44	1.01 ± 0.46		
NO^{-3} (kg)	0.21 ± 0.10	0.18 ± 0.05		
TP (kg)	0.04 ± 0.01	0.03 ± 0.02		
Barium (kg)	0.01 ± 0.005	0.06 ± 0.02		
Zinc (kg)	0.15 ± 0.15	0.13 ± 0.12		
E. coli (Billion MPNs)*	57± 27	4 ± 2		

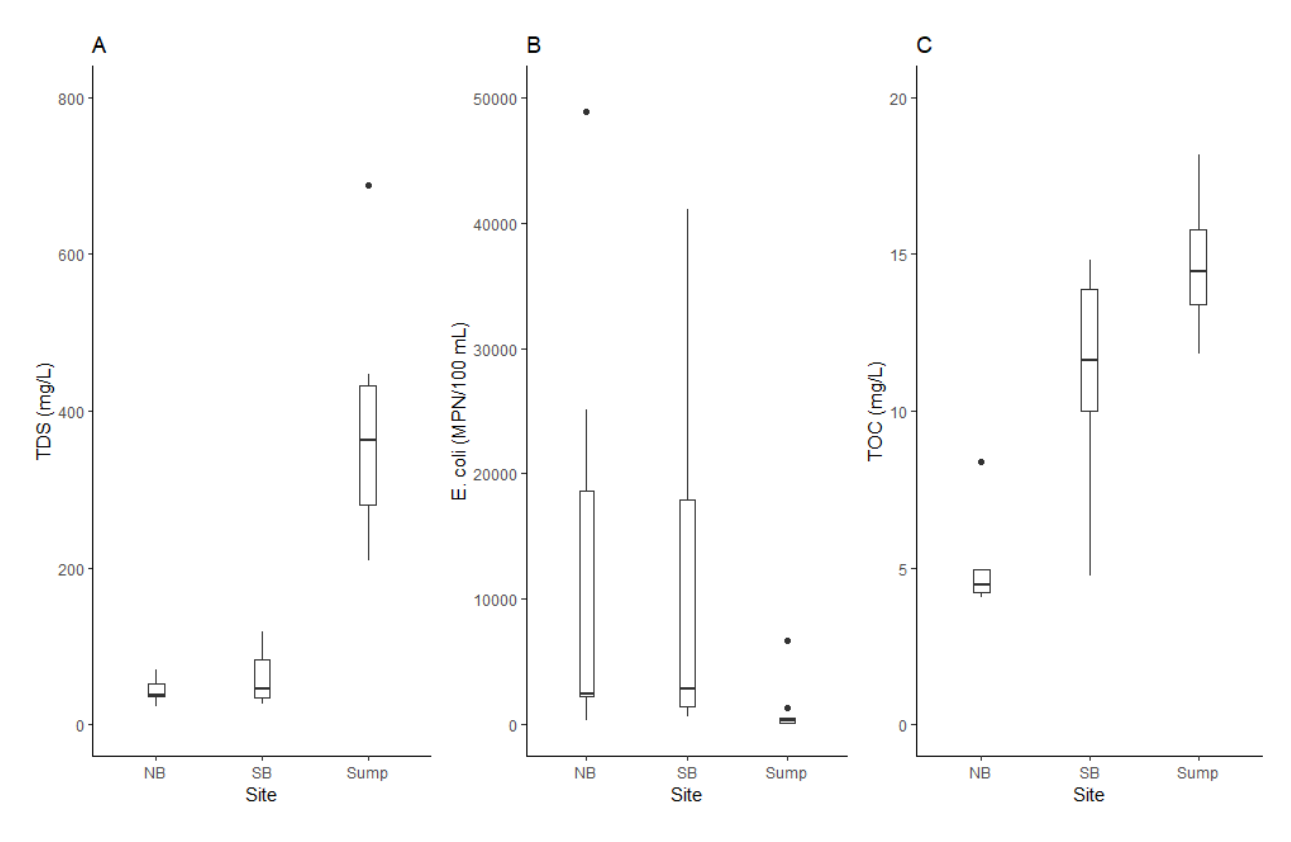


Figure 20. Distributions of analyte event mean concentrations that showed significant differences from north basin (NB) or south basin (SB) inputs to sump outlet in the bioretention basin. Measures of A) total dissolved solids (TDS) increased in the sump outlet compared to both basins, measures of B) E. coli decreased in the sump outlet compared to both basins, and measures of C) TOC increased in the outlet compared to the north basin.

Post-construction temperature

Temperature data was only available for the basins for flow events from 14 October 2021 to 17 December 2021, due to inconsistent data retrieval and early issues with temperature loggers malfunctioning during long periods of submergence in the basins and sump outlet. Temperature spikes were observed in both basins during all four events monitored, averaging 4.2 F in the north basin and 4.0 F in the south basin, slightly higher on average than pre-temperature spikes. Unfortunately, matched temperature data for the sump outlet was not available to determine whether temperature spikes were muted as water moved through the bioretention basin. However, temperature records from the basins provide some evidence that temperature spikes were likely muted. In all four events, water temperatures in the basins quickly receded from the initial spike and usually maintained temperatures lower than the peak, even as air temperature increased (Figure 21). Given that the temperature spike was alleviated over time in the basins, the spike was likely muted in water leaving the sump outlet.

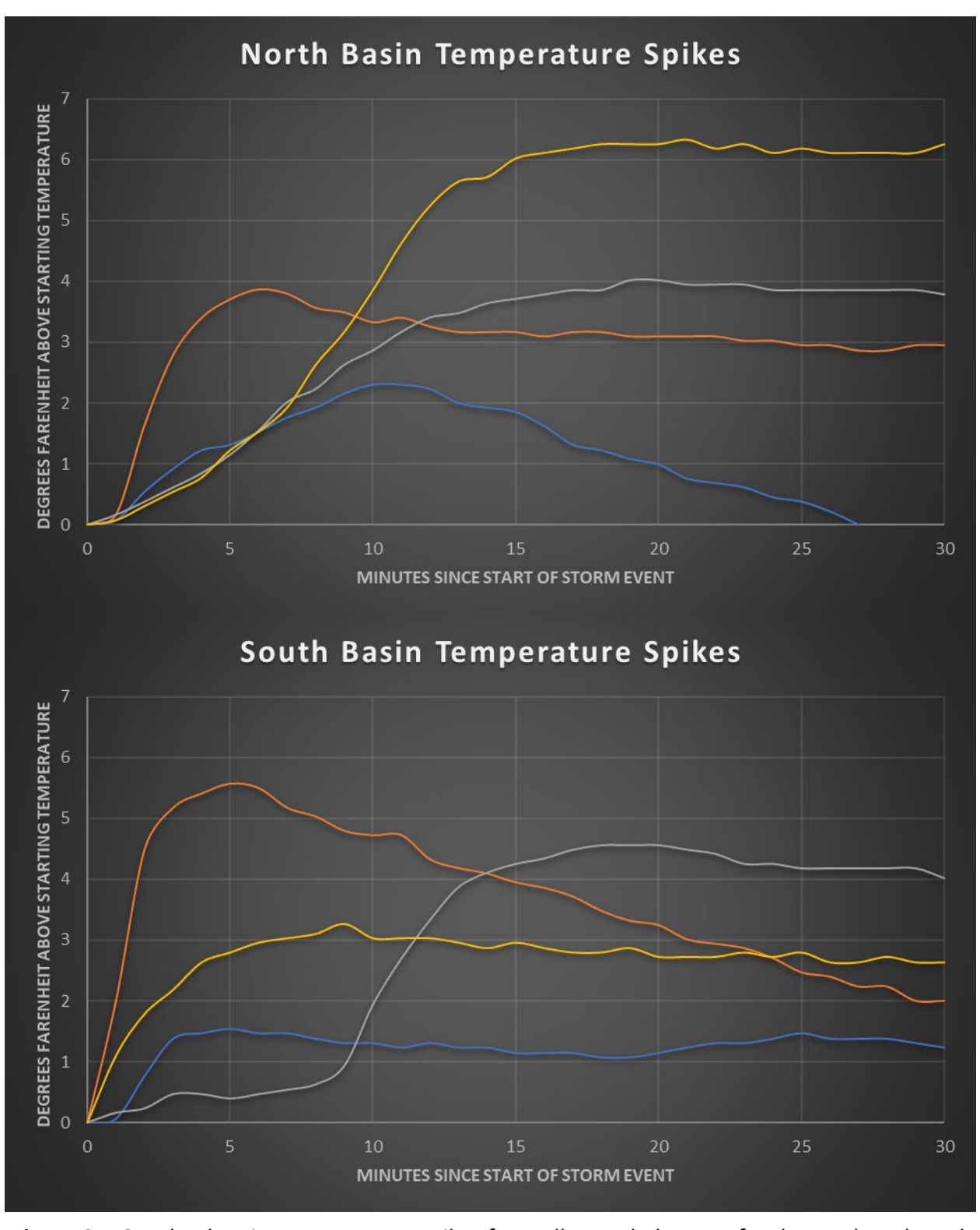


Figure 21. Graphs showing temperature spikes from all recorded events for the north and south basin post-construction. Note that most events show at least a slight decline from the peak temperature, though several show a subsequent warming trend.

Discussion

In 2017, funding was provided through the City of San Antonio's Edwards Aquifer Protection Venue Program to retrofit with LID facilities, 9.7 acres of impervious cover on the University of Texas at San Antonio main campus. The goal of implementing the facilities was to reduce peak flow volumes and pollutant transport downstream during runoff events on the campus. In addition, the project aimed to improve the aesthetic environment of a central campus location and provide educational opportunities for university students and campus visitors. The LID facilities installed included cisterns, a bioretention basin, a grassy channel and a bioswale, connected through flow pathways in a treatment train approach. To determine the effectiveness of the bioretention basin in reducing peak flow volumes and pollutant transport downstream, a study was undertaken in which flow and water quality was monitored in an upstream and downstream location pre- and post-construction. Here we discuss aesthetic changes made to the campus environment as a result of LID facility construction and the performance of the bioretention basin with respect to capturing runoff and filtering pollutants during storm events. A separate business plan discusses cost considerations and recommendations for LID facility implementation on other university campuses or similar environments.

Changes to campus environment

Installation of the LID facilities substantially altered the landscape of a central campus green space. The primary area that changed was the bioretention basin, though changes were also made to the grassy channel and bioswale. The location where the bioretention basin was constructed was a maintained lawn with patches of live oak trees and a storm conveyance channel running through the center (Figure 4). After construction, the same area consisted of two basins separated by an earthen berm, with trees that existed prior to construction maintained and additional native vegetation planted in and around the berms (Figure 4). The construction was completed in November 2020 and after two years, the native plants have grown in as intended in the landscaping plans (Figure 15). The space received minimal use prior to construction, primarily serving as an unofficial pathway between buildings and hosting a few campus events on the lawn each year. The space is now a functioning LID facility, providing a landscaped environment, including a space with chairs and power outlets for study or relaxation, and serving as a temporary water feature after runoff events. In addition, signs placed at the bioretention basin inform students and visitors about the LID facility and the importance of managing stormwater runoff for downstream aquatic environments, including the Edwards Aquifer. The bioswale, though smaller than the bioretention basin, also provided a similar alteration to a previously existing mowed grassy channel (Figure 7). A heavily trafficked footpath parallels the bioswale and unmowed grassy channel and an informational sign is also installed at this location, making these highly visible LID facilities.

Hydrologic effectiveness

Comparison of estimated hydrographs with and without the bioretention basin indicated a substantial reduction in peak flow volume in the channel downstream of the bioretention basin. The constructed basins of the bioretention system were estimated to hold 374,000 gallons of water, and maximum peakflow rates were anywhere from 0.5 to 20 times lower with the basins installed compared to without the basins installed, depending on the storm event. In the pre-construction condition, all runoff from the upstream watershed was conveyed downstream in the existing channel rapidly. Storm events passed through the preconstruction channel in an average of approximately 3 hours. Water level monitoring in the basins showed that water ponded in both the north and south basins and infiltrated into the basin soils as intended. Estimated hydrographs of discharge from the bioretention basin indicated the basins were releasing water downstream over a period of several days, much slower compared to the pre-construction phase. Adding the 19,000 gallon capacity of the cisterns to the capacity of the bioretention basin, the LID facilities represent a significant storage of water and attenuation of peakflows downstream compared to the pre-construction condition. However, it should be noted that there is a limited capacity of water storage, such that large events will not be substantially attenuated, and approximately four events of such magnitude did occur during the post-construction monitoring period from February 2021 to February 2022.

Water quality treatment

Stormwater runoff from the study watershed contained fairly low concentrations of most pollutants. For example, pesticides, herbicides, total petroleum hydrocarbons (TPH), and many metals such as lead and mercury were never detected or rarely found in detectable concentrations. Total phosphorus (TP) was also frequently at concentrations below detection limits. One pollutant that was found in high concentrations in stormwater runoff was *E. coli*, which was frequently found at concentrations > 1,000 MPN/100mL in untreated stormwater. Elevated *E. coli* concentrations may have resulted from animal activity, including feral cats, which used walkway tunnels upstream of the bioretention basin as shelter, though more research would be needed to positively identify major sources.

Despite low concentrations for many pollutants, results indicated the bioretention basin was effective at treating several pollutants, including *E. coli*, total suspended solids (TSS), nitrate (NO₃-), TP, and copper. The strongest impacts were seen for *E. coli*, which was reduced by >75% in terms of first flush and event mean concentrations for both the north and south basin, and, importantly, showed a significant decrease in total load from water coming into the bioretention basin compared to water leaving the basin. Comparable data for the preconstruction channel were not collected, so there is a possibility that a similar treatment of *E. coli* was occurring prior to implementation of the bioretention basin. However, this is unlikely given that the pre-construction condition was a simple mowed grass channel and no load reductions were seen pre-construction for any other analyte tested.

The north basin had higher first flush concentrations of several analytes compared to the south basin, including TSS and NO₃-, possibly due to the south basin receiving water mostly from the Convocation Center rooftop, whereas the north basin received water from upstream parking lots and roadways in addition to runoff from the HEB Student Union. These different inputs of water were also likely causing increases of some analyte concentrations from site A to site B in the pre-construction channel, including TDS, TOC, and copper. The bioretention basin reduced first-flush concentrations of TSS in the north basin by 13% on average. A similar reduction in first-flush concentrations was seen upstream to downstream in the preconstruction channel. Reductions in the pre-construction channel may have been caused by dilution, since flow increased from the upstream to downstream location, and a similar effect may have occurred in the bioretention basin, since TSS first flush concentrations were not different between the south basin and sump outlet. In addition, TSS concentrations were highly variable between events in post-construction monitoring, with especially high concentrations in the north basin and sump outlet during the first sampled storm event. High concentrations in the first monitored event in the sump outlet may have been caused by sediment washing out of piping after the construction phase. Whatever the cause, the highly variable measurements of TSS make the effectiveness of the TSS removal capacity of the bioretention basin somewhat uncertain. There is stronger evidence that the basin was treating NO₃ effectively, because first flush concentrations of NO₃ were lower in the sump outlet compared to the north basin, whereas concentrations were frequently higher in the downstream location pre-construction. Nonetheless, dilution could still be a contributing factor to reduced NO₃- concentrations, since the south basin first flush concentrations were not significantly different from the sump outlet concentrations.

First flush concentrations of copper and TP were found at detectable levels much less frequently in the sump outlet compared to basin inlets, with the infrequent detections limiting power for statistical testing. Neither analyte showed a decrease in first flush concentrations pre-construction, and particularly for copper, the lack of detections in the sump outlet suggest a likely load reduction, though this could not be tested statistically. The relatively low concentrations of many analytes may have precluded statistical detection of significant load reductions in the bioretention basin, especially since the pollutant found at highest concentrations, *E. coli*, showed a marked decrease. Another potential source of error in calculating loads was the inability to distinguish individual storm events in the sump outlet flow record. Since we assumed the same flow volume in the input and outlet of the basins, whereas outlet flow volume was likely lower due to evapotranspiration, our estimates of load changes were biased toward not finding significant load reductions. Thus, it is possible other analytes would have shown load reductions with better outlet flow data, but based on event mean concentrations, the outlet flow volume would have to be at least 60% lower for any other analytes to show significant load reductions.

Temperature monitoring demonstrated a likely attenuation of temperature spikes during runoff events, though more data will be needed to confirm the result. Temperature

spikes, defined by a sharp increase in water temperature during the first flush of a runoff event, were observed in all runoff events in the pre-construction channel and in the water flowing into the bioretention basins. The spike magnitude, defined as the difference in temperature between the max temperature of the spike and the air temperature at the start of the runoff event, averaged approximately 4 F across all observed temperature spikes. Temperature monitoring in the bioretention basins showed a quick attenuation of the initial temperature spike as water accumulated in the basins during the course of a runoff event. Water accumulated in the basins subsequently infiltrated slowly into the basin soils, eventually flowing in the basin underpiping to the sump outlet. This delayed movement of the runoff water downstream suggests the temperature spike was attenuated in water pumped out of the basin, though lack of temperature data for the sump outlet currently prohibits confirmation of this result. Although the temperature spike may be attenuated, water ponded in the basins also steadily increased in temperature during warm days, suggesting the average temperature of water pumped out of the basin may be higher than in the pre-construction condition, but movement through basin soils could counteract this effect. Temperature monitors are being maintained in the basins and sump outlet, and data should be available soon to further investigate the effect of the bioretention basin on water temperatures.

Concentrations of several analytes in the sump outlet water were higher than concentrations coming into the bioretention basin, including total dissolved solids (TDS), total organic carbon (TOC), barium, and arsenic. The increase in concentration of TDS was sufficient to cause a statistically significant increase in total load in the outlet water as well. Increases in TDS have been observed in other bioretention basins, as indicated by monitoring of other bioretention basins on the UTSA campus and personal communication with other stormwater management professionals, suggesting the increase is a common phenomenon. Potential causes of the TDS increase are leaching of salts from bioretention basin soils or high microbial activity and breakdown of organic matter, the latter explanation partly supported by an observed increase in TOC concentrations in the basin outlet water, at least compared to the north basin. Concentrations of TDS in basin outlet water are not considered problematic, because they are generally below levels considered harmful for aquatic life. The source of increases in barium and arsenic concentrations are not known definitively, but basin soils are a likely source. Barium is not considered problematic, because concentrations are well below levels considered harmful and loads did not increase significantly. Arsenic is of potential concern, as some concentrations were slightly in excess of drinking water standards and loads could not be tested due to limited detections in basin inlet water. Further study of sump outlet water and basin soils may be warranted to better understand sources of arsenic and whether concentrations remain at detectable levels over longer time periods. If further studies show arsenic to be an issue, future construction projects may want to consider testing bioretention basin material for arsenic contamination.

Conclusions

Key questions addressed by the construction of LID facilities and the hydrologic and water quality monitoring were whether the LID facilities were effective in retaining stormwater runoff and removing pollutants from runoff compared to a mowed grassy channel that existed prior to LID facility construction, and whether the LID facilities could be incorporated as an aesthetic green feature in a highly trafficked area of the UTSA campus. The LID facilities were successfully integrated as functional green spaces into the campus environment, serving to provide stormwater retention, water filtering capacity, unique landscape features, and educational opportunities. The bioretention basin in particular transformed a lightly used lawn and storm conveyance channel into two basins planted with multiple species of native vegetation that serve as temporary water features after storm events occur. A downstream bioswale provided a similar transformation, though on a smaller scale. The bioretention basin successfully captured stormwater runoff, with a total capacity estimated at 374,000 gallons, and allowed the water to infiltrate into basin soils rather than being conveyed immediately downstream in the former grassy channel. By holding water and releasing it more slowly, the basin substantially attenuated downstream peakflows. Two cisterns with a total capacity of 19,000 gallons further increased stormwater retention and provided irrigation water for campus. The bioretention basin significantly reduced loads of E. coli bacteria, reduced first-flush concentrations of TSS, copper, and nitrate, and likely attenuated temperature spikes relative to the pre-construction grassy channel. Some concerns regarding increases of some water quality constituents in the bioretention basin, particularly arsenic, may warrant further investigation. However, water leaving the basin enters additional LID facilities as part of the treatment train implementation, providing potential further water quality improvement. Signs emplaced near each LID facility inform students and campus visitors about the LID facilities and how they help to protect aquatic resources, such as the Edwards Aquifer. A partner document in the form of a business plan discusses lessons learned and potential viability regarding how the observed benefits can be replicated on other campus environments.

Acknowledgements

We thank the City of San Antonio for providing funding and personnel with the San Antonio River Authority for helpful guidance throughout the project. Many graduate and undergraduate students assisted with sample collection and analysis, especially H. Escobar, A. Adeyeye, and E. VonBon.

References

Andrews, F., Schertz, T., Slade, R. J., & Rawson, J. (1984). Effects of storm-water runoff on water quality of the Edwards Aquifer near Austin, Texas. *Water-Resources Investigations Report*, 84, 4124.

- Arnold, C. L., Boison, P. J., & Patton, P. C. (1982). Sawmill Brook: An example of rapid geomorphic change related to urbanization. *The Journal of Geology*, *90* (2), 155–166. https://doi.org/10.1086/628660
- Bannerman, R. T., Owens, D. W., Dodds, R. B., & Hornewer, N. J. (1993). Sources of pollutants in Wisconsin stormwater. *Water Science and Technology*, *28* (3-5), 241–259. https://doi.org/10.2166/wst.1993.0426
- Bowles, D. E., & Arsuffi, T. L. (1993). Karst aquatic ecosystems of the Edwards Plateau region of central Texas, USA: A consideration of their importance, threats to their existence, and efforts for their conservation. *Aquatic Conservation: Marine and Freshwater Ecosystems*, 3, 317-329.
- Brabec, E., Schulte, S., & Richards, P. L. (2002). Impervious surfaces and water quality: A review of current literature and its implications for watershed planning. *Journal of Planning Literature*, 16 (4), 499-514. https://doi.org/10.1177/088541202400903563
- Gwinn, D. C., Middleton, J. A., Beesley, L., Close, P., Quinton, B., Storer, T., & Davies, P. M. (2018). Hierarchical multi-taxa models inform riparian vs. hydrologic restoration of urban streams in a permeable landscape. *Ecological Applications*, 28 (2), 385–397. https://doi.org/10.1002/eap.1654
- Huber, M., Welker, A., & Helmreich, B. (2016). Critical review of heavy metal pollution of traffic area runoff: Occurrence, influencing factors, and partitioning. *The Science of the Total Environment*, *541*, 895–919. https://doi.org/10.1016/j.scitotenv.2015.09.033
- Leopold, L. B. (1968). Hydrology for urban land planning: A guidebook on the hydrologic effects of urban land use. U.S. Geological Survey Circular 554, Washington, DC.
- Masoner, J. R., Kolpin, D. W., Cozzarelli, I. M., Barber, L. B., Burden, D. S., Foreman, W. T., Forshay, K. J., Furlong, E. T., Groves, J. F., Hladik, M. L., Hopton, M. E., Jaeschke, J. B., Keefe, S. H., Krabbenhoft, D. P., Lowrance, R., Romanok, K. M., Rus, D. L., Selbig, W. R., Williams, B. H., & Bradley, P. M. (2019). Urban stormwater: An overlooked pathway of extensive mixed contaminants to surface and groundwaters in the United States. *Environmental Science & Technology*, *53* (17), 10070–10081. https://doi.org/10.1021/acs.est.9b02867
- McGrane, S. J. (2016). Impacts of urbanization on hydrological and water quality dynamics, and urban water management: a review. *Hydrological Sciences Journal*, *61* (13), 2295-2311. https://doi.org/10.1080/02626667.2015.1128084
- Morisawa, M., & LaFlure, E. (1979). Hydraulic geometry, stream equilibrium and urbanization. In D. D. Rhodes & G. P. Williams (Eds.), Adjustments of the fluvial system (pp 333-350). London: Routledge.

- Musgrove, M., Opsahl, S. P., Mahler, B. J., Herrington, C., Sample, T. L., & Banta, J. R. (2016). Source, variability, and transformation of nitrate in a regional karst aquifer: Edwards aquifer, central Texas. *Science of the Total Environment*, *568*, 457-469. https://doi.org/10.1016/j.scitotenv.2016.05.201
- Paul, M. J., & Meyer, J. L. (2001). Streams in the urban landscape. *Annual review of Ecology and Systematics*, 32 (1), 333-365.
- Pitt, R., Maestre, A., & Morquecho, R. (2004). *The national stormwater quality database (NSQD, version 1.1).* Paper presented at the 1st Annual Stormwater Management Research Symposium Proceedings.
- San Antonio River Authority (SARA). (2019). San Antonio River Basin low impact development technical guidance manual, v2. San Antonio, TX: San Antonio River Authority.
- Texas Commision for Environmental Quality. (2022). Prepared by TCEQ Water Availability Division, Groundwater Assessment 2022 State of Texas Water Quality Inventory, TCEQ AS-465/22 April 2022